N73-21072

NASA TECHNICAL MEMORANDUM

NASA TM X-2758

NASA TM X-2758

CASE FILE COPY

SMALL-SCALE NOISE TESTS OF A SLOT NOZZLE WITH V-GUTTER TARGET THRUST REVERSER

by James R. Stone and Orlando A. Gutierrez

Lewis Research Center

Cleveland, Ohio 44135

NATIONAL AERONAUTICS AND SPACE ADMINISTRATION • WASHINGTON, D. C. • APRIL 1973

1. Report No. NASA TM X-2758	2. Government Accession No.	3. Recipient's Catalog No.
4. Title and Subtitle SMALL-SCALE NOISE TESTS OF A SLOT NOZZLE WITH V-GUTTER TARGET THRUST REVERSER		5. Report Date April 1973
		6. Performing Organization Code
7. Author(s) James R. Stone and Orlando A. Gutierrez		8. Performing Organization Report No. E-7307
		10. Work Unit No. 501-24
9. Performing Organization Name and Address Lewis Research Center National Aeronautics and Space Administration Cleveland, Ohio 44135		11. Contract or Grant No.
		13. Type of Report and Period Covered Technical Memorandum
12. Sponsoring Agency Name and Address National Aeronautics and Space Administration Washington, D. C. 20546		14. Sponsoring Agency Code
15. Supplementary Notes		

16. Abstract

This report presents the results of experiments on the noise generated by a 2.26- by 11.43-cm slot nozzle with a V-gutter reverser, as well as some aerodynamic data on flow, thrust-reversal efficiency, and nozzle jet velocity decay. The experimental data are scaled up to sizes suitable for reversing the wing flow of a 45 400-kg augmentor-wing-type STOL airplane, yielding perceived noise levels well above the 95-PNdB design goal on the 152-m sideline. The reverser, in addition to being noisier than the nozzle alone, also had a more uniform directional distribution and more high-frequency noise. The maximum overall sound pressure level and the effective sound power level both varied with the sixth power of nozzle jet velocity. Preliminary experiments indicated possible sideline noise reduction by shielding.

17. Key Words (Suggested by Author(s))		18. Distribution Statement
Thrust reversers	Acoustic	Unclassified - unlimited
Noise level	Experimental	
STOL aircraft		

19. Security Classif. (of this report)	20. Security Classif. (of this page)	21. No. of Pages	22. Price*
Unclassified	Unclassified	64	$3.00

* For sale by the National Technical Information Service, Springfield, Virginia 22151

SMALL-SCALE NOISE TESTS OF A SLOT NOZZLE WITH V-GUTTER TARGET THRUST REVERSER

by James R. Stone and Orlando A. Gutierrez

Lewis Research Center

SUMMARY

This report presents the results of experiments on the noise generated by a 2.26- by 11.43-centimeter slot nozzle with a V-gutter target thrust reverser. Some aerodynamic data on flow, thrust reversal efficiency, and nozzle jet velocity decay are also presented. The experimental data are scaled up to sizes suitable for reversing the wing flow of a 45 400-kilogram augmentor-wing-type STOL airplane. These scaling calculations yield perceived noise levels well above the 95-PNdB design goal on the 152-meter sideline.

The noise data are compared with data for a V-gutter reverser with a circular nozzle; the overall sound pressure levels and overall sound power levels agreed well, but the spectral distributions were somewhat different. Like the target reversers tested with circular nozzles, the reverser tested herein, in addition to being noiser than nozzles alone, also had a more uniform directional distribution and more high-frequency noise. The maximum overall sound pressure level and the effective sound power level both varied with the sixth power of nozzle jet velocity, as was also the case for the target reversers tested with circular nozzles. Preliminary experiments indicated possible sideline noise reduction by shielding.

INTRODUCTION

Since STOL aircraft are intended to operate from airports in heavily populated areas, they will be required to meet much stricter noise regulations than conventional aircraft. For this reason, the Lewis Research Center has recently conducted several studies on the noise generated by STOL propulsion system components (e.g., refs. 1 to 7). In order to achieve the goal of landing in short distances, jet STOL aircraft may well employ thrust reversers, both for reducing the ground roll after landing and for steepening the approach flightpath. As an example, for the augmentor-wing-type airplane, high thrust is required through the wing air-distribution system to maintain high

lift during approach. Thus, complete or partial in-flight reversal of the core jets is an alternative being considered as a means of reducing airspeed during descent. Reference 1 presents noise data for core-jet target thrust reversers, and reference 2 gives the normalization of these data and the scale-up to sizes suitable for reversing the core jets of a 45 400-kilogram augmentor-wing-type airplane. These scale-up calculations indicate perceived noise levels well above the 95-PNdB design goal for both sideline and flyover at 152 meters.

For reducing the ground roll of an augmentor-wing-type airplane, however, the wing flow must be reversed, since its thrust is much greater than that of the core jets. Both slot and multielement nozzles are being considered for supplying the airflow to the augmentor flaps. Engines mounted above the wings have recently been proposed for the externally-blown-flap STOL configuration; such engines might well employ short-aspect-ratio slot nozzles equipped with target thrust reversers. Therefore, information on the noise generating characteristics of thrust reversers for slot nozzles is required.

There have been many studies of the aerodynamic performance of small-size thrust reversers of diverse types (e.g., refs. 8 to 10). Reports are also numerous on the behavior of full-scale reversers (e.g., refs. 11 to 14). Although it is apparent from the preceding references that the aerodynamic behavior of reversers has been extensively studied and documented, this has not been the case with regard to noise.

A V-gutter target-type reverser was chosen for this study, since such a configuration could be used with the augmentor-wing slot and flap system, as shown in figure 1. A V-gutter reverser might also be used with the short-aspect-ratio slot nozzles which are being considered for the engine-over-the-wing externally-blown-flap concept (refs. 3 and 4). The slot nozzle used was 11.43 centimeters long and 2.26 centimeters high, with the ends rounded; this nozzle was also used in references 3 and 4. The nozzle area is essentially the same as that of the circular nozzle of references 1 and 2. The nozzle jet velocity ranged from 190 to 390 meters per second. The effects of the spacing between nozzle and reverser and the offset of the reverser centerline from the nozzle centerline are reported. Plywood shields were used to block off the sound radiated from various sections of the jet, thus giving some indication of the location of noise sources. These tests also indicated that some sideline noise reduction might be obtained by shielding. Scale-up calculations for reversing the wing flow of a 45 400-kilogram augmentor-wing-type airplane indicated perceived noise levels in excess of the 95-PNdB design goal on the 152-meter sideline.

APPARATUS AND PROCEDURE

The experimental data were obtained on two separate flow systems. The noise data

were taken on an acoustic rig designed to minimize internal noise and instrumented to obtain detailed acoustic data. Another airflow rig was used to obtain slot-nozzle jet velocity surveys and data on flow and thrust-reversal efficiency.

Acoustic Rig

The acoustic rig is shown in figure 2. Compressed air from a 1000-kN/m^2 abs source was supplied to the nozzle at near ambient temperature by a 10-centimeter-nominal-diameter pipe. This pipe was equipped with a flow-measuring orifice, a hand-operated flow-control valve, a noise muffler, and a straight run ending at the nozzle. The pipe was 1.63 meters above ground level. The thrust reverser was mounted on a rack attached to the air supply pipe, as shown in figure 2.

The noise data were measured by condenser microphones with individual wind screens, located on a 3.05-meter-radius circle centered on the nozzle exit. Eight to 11 microphones were used, depending on the experiment. The microphone circle was at nearly the same height from the smooth asphalt surface as the nozzle centerline, 1.6 meters. The microphones were set at 20° intervals from 20° to 160° for all cases including the nozzle alone; with the reverser a microphone was added at 180°. For the shielding experiments, microphones were also placed at 260° and 280°. The upstream axis of the nozzle was at $\theta = 0^\circ$, and $\theta = 180^\circ$ is the extension of the pipe axis downstream of the nozzle. (Symbols are defined in appendix A.)

Airflow Rig

The airflow rig, described in more detail in reference 15, is shown in figure 3 with the slot nozzle and V-gutter reverser installed. This rig was used to obtain data on flow, thrust-reversal efficiency, and nozzle jet velocity decay; but, since the rig was located in a relatively small nonacoustic chamber, no noise measurements were made. Pressurized air flowed to the nozzle through a nominal 15-centimeter pipe, to which the air was fed by two diametrically opposed supply lines. Flexible couplings in each of these two supply lines isolated the supply system from the force-measuring system. A 2.2-kilonewton full-scale load cell was used to measure thrust. The cell was preloaded with weights hung from pulleys to measure reverse thrust. The airflow rate was measured with an orifice.

Free-jet surveys downstream of the nozzle, with the thrust reverser and mounting rack removed, were made with a traversing pitot-static probe at several stations downstream of the nozzle exit. The measurements from the traversing probe were trans-

mitted to an x-y-y' plotter which gave direct traces on graph paper of the total- and static-pressure distributions across the jet.

Nozzle and Reverser

Nozzle. - The slot nozzle used in these studies and in references 3 and 4 is sketched in figure 4. The nozzle consists of a transition from an upstream circular cross section of nominal 10-centimeter diameter to the 11.43-centimeter-long by 2.26-centimeter-high slot with rounded ends. This transition is accomplished over an axial distance of 24 centimeters. Some of the pertinent dimensions are

Slot height, H_n, cm	2.26
Average slot length, $\overline{W}_n = A_n/H_n$, cm	10.77
Slot area, A_n, m^2	2.43×10^{-3}
Aspect ratio, $\overline{W}_n/H_n$	4.76
Hydraulic diameter, D_h, cm	3.79
Equivalent circular diameter, D_e, cm	5.56

Reverser. - The V-gutter thrust reverser used in these studies is sketched in figure 5. The reverser was made from a section of nominal 7.5 centimeter steel angle; the flow was channeled by two 0.8-millimeter-thick aluminum-sheet end plates. The reverser frontal area was 0.01245 square meters.

Arrangement of nozzle and reverser. - The arrangement of the reverser with respect to the nozzle is sketched in cross section in figure 6, and pertinent dimensions are defined. Both reverser surfaces were at 45^o to the nozzle axis. In only two acoustic runs was the offset Y_0 other than zero, and in only one acoustic run was the spacing X other than -0.64 centimeter (overlapped by 0.64 cm). The ratio of reverser frontal area to the nozzle area was 5.12. The larger of the two perpendicular distances from the reverser to the nozzle outer lip H_R (dimensions in m) is

$$H_R = 0.0221 + 0.707 (X + Y_0) \tag{1}$$

The distance from the back of the reverser to the nozzle exit plane L is given by

$$L = 0.0312 + X \tag{2}$$

Sideline shield. - Plywood sheets were used to shield portions of the jet from various microphones in order to get some indication of the location of noise sources and to get some information on possible sideline noise reduction by shielding. One

1.3-centimeter-thick plywood sheet, 61 centimeters wide, was attached to the outside of the reverser mounting rack (fig. 2); thus, the 60° to 120° microphones were shielded. The board extended from the center of the "V" almost to the ground. A second 61-centimeter-wide board was used to raise the top of the shield to various distances above the center of the "V". One run was made with the entire shield moved 15.2 centimeters forward, thus shielding the microphones at 40° to 100° and partially unshielding the 120° microphone from the edge of the reverser.

Procedure

During the acoustic tests, some aspects of shielding and acoustic treatment were investigated. Plywood shields were fastened to the reverser mounting rack at various positions to shield the sideline from different parts of the flow field. Adding acoustic treatment to the back of the reserver had no effect, so data taken with and without treatment can be compared directly.

The range of reverser-to-nozzle spacings for the acoustic tests was estimated based on literature data for circular nozzles. However, after the acoustic tests, aerodynamic data for the acoustic test conditions and other cases of interest were obtained on the airflow rig. Data on both flow and thrust were obtained.

For comparative purposes, acoustic, flow, and thrust data were obtained for the nozzle alone. Also, velocity survey data for the nozzle alone were obtained on the airflow rig

Experimental procedure. - For each acoustic run, the nozzle-reverser combination was set at the proper spacing and orientation, and any shields to be used were clamped into place. Flow of unheated compressed air was established and regulated by the hand-operated throttle valve. The controlled parameter was the nozzle inlet pressure P_n. After flow conditions stabilized, flow parameters and atmospheric conditions were recorded and three noise data samples were taken for each microphone. These noise data were analyzed directly by a 1/3-octave-band spectrum analyzer. The analyzer determined, for each microphone and sample, the sound pressure level (SPL) for each 1/3-octave band from 50 to 20 000 hertz. This information was placed on tape for computer processing. The microphones were calibrated at the start and end of each day's operation with a standard piston calibrator.

Noise data analysis. - The spectral sound-pressure-level data from the 1/3-octave-band analyzer were corrected for atmospheric absorption and averaged to eliminate gross errors. The sound pressure levels were 3 dB above free-field values except for those frequency bands exhibiting cancellations and reinforcements: no corrections to free-field values were made in this report. With the microphones on a 3.05-meter-

radius circle and 1.63 meters above the ground, cancellations should occur in the 125-, 400-, and 630-hertz bands, assuming a point noise source also at a height of 1.63 meters; reinforcements should occur in the 250-, 500-, and 800-hertz bands. At higher frequencies, cancellations and reinforcements occur within the same band, and so have little effect. The averaged values of SPL for each microphone were then added antilogarithmically to obtain the overall sound pressure level (OASPL). Except for the data from the shielding tests, the effective spectral sound power level (PWL) and the effective overall sound power level (OAPWL) were then calculated from the SPL data. The integration is performed only over one hemisphere since the sound pressure levels were assumed to be 3 dB above free-field values except for those bands affected by cancellations and reinforcements. In principle, the noise measured may be a function of the angle of the microphone plane to the reverser, and the data are for one plane only; hence, these power levels are termed "effective." It should be noted that rotating the reverser and nozzle 90° had very little effect on the effective power levels as discussed later in the report, but no data were obtained at intermediate angles.

RESULTS AND DISCUSSION

The experimental test conditions and major results are given in table I; the detailed acoustic data are given in table II. For the acoustic tests, the reverser was spaced far enough from the nozzle that the flow rate was not decreased by the presence of the reverser; relatively high thrust-reversal efficiency should thereby be obtained. The effects of spacing on flow rate and thrust-reversal efficiency are presented in appendix B. Appendix C presents jet velocity survey data for the slot nozzle without the reverser.

Reversed flow patterns obtained during the tests were observed. The flow exited along the plates forming the V and then attached to the outside of the nozzle. Only an insignificant amount of flow left the reverser along the end plates. All the nozzle flow was captured and reversed.

Effect of Thrust Reversal on Noise

The effects of thrust reversal on the directivity pattern and spectral distributions of sound pressure level on the 3.05-meter radius and on the effective sound power level are shown in figures 7, 8, and 9. The leading edge of the reverser overlapped the nozzle by 0.64 centimeter, and the orientation of the reverser was horizontal. Data are plotted for nozzle jet velocities of 190, 285, and 360 meters per second in parts (a), (b), and (c), respectively, in each figure. The highest velocity is slightly supersonic. (The 190-m/

sec data for the nozzle alone were obtained by adding 2 dB to the data obtained at 179 m/sec, assuming a variation of SPL and PWL with the eighth power of the nozzle jet velocity.)

Directivity. - Figure 7 shows the overall sound pressure level (OASPL) as a function of angular position from the nozzle upstream axis θ. Subsonically (figs. 7(a) and (b)), the nozzle alone has a maximum OASPL at 160°; and its minimum OASPL, which occurs at $\theta = 20^{\circ}$, is lower by 9 or 10 dB. Thus, the slot nozzle directional effects are fairly strong, though not quite so strong as for the circular nozzle of reference 1. With the reverser, at the lowest velocity (190 m/sec (fig. 7(a)), the maximum OASPL, at $\theta = 20^{\circ}$, is about 16 dB above that of the nozzle alone; while the minimum OASPL is only about 7 dB less than the maximum. At 285 meters per second, the reverser maximum OASPL is shifted slightly to 40° and is 10 dB above that of the nozzle alone; the minimum OASPL is about 8 dB less than the maximum. The directional effects with the reverser are somewhat greater than those of the reversers tested in reference 1, but they are still less than those of the slot nozzle alone. For the supersonic case (fig. 7(c)), the situation for the nozzle alone is complicated by broad-band shock noise and discrete tones, or "screech"; the maximum OASPL is at 140°, while the minimum OASPL is 12 dB less and occurs at 40°. The supersonic data with the reverser are similar to those at lower velocities, with no apparent shock noise or screech; and the maximum OASPL with the reverser is only about 1 dB greater than that of the nozzle alone.

Sound pressure level spectra. - Figure 8 shows the sound pressure level (SPL) as a function of the 1/3-octave-band center frequency f_c at the angle of maximum overall sound pressure level. The frequency bands affected by discrete ground-reflection cancellations and reinforcements are labeled C1, C2, C3 and R1, R2, R3, respectively; the fourth cancellation and reinforcement both occur within the 1-kilohertz band. None of these ground reflections seem to affect the data much, except the first reflection at 250 hertz; the peak at 125 hertz, where the first cancellation should occur, is caused by background noise. The supersonic data for the nozzle alone show the 2- and 4-kilohertz bands to be affected by screech; the otherwise relatively flat and high-amplitude high-frequency spectrum is characteristic of broand-band shock noise. For all cases, the peak SPL occurs at higher frequency with the reverser than with the nozzle alone. This reverser configuration also gave a flatter and higher-frequency peak than the V-gutter reverser and circular nozzle configuration (ref. 1), which had a fairly sharp peak at 1250 hertz.

Sound-power-level spectra. - Figure 9 shows the sound power level (PWL) as a function of the 1/3-octave-band center frequency f_c. Because of the background noise problem mentioned in the previous paragraph, power levels were not computed for less than 250 hertz with the reverser. Ground-reflection cancellations and reinforcements are indicated as in the preceding figure; the effects are generally noticeable but small,

except for the relatively strong 250-hertz reflection. The effect of thrust reversal is fairly well defined here: the reverser has no significant effect on the low-frequency noise; but the reverser generates more noise at high frequencies, with the differences in high-frequency spectra decreasing with increasing velocity. Again, this reverser configuration gave a flatter and higher-frequency peak than the V-gutter reverser and circular nozzle (ref. 1), which had a fairly sharp peak at 1250 hertz. The supersonic case is again complicated for the nozzle alone by broad-band shock noise and screech at 2, 4, and 8 kilohertz. To eliminate the shock effects in an approximate way, the subsonic data were normalized to a U_j of 360 meters per second, assuming $10^{PWL/10} \propto U_j^8$ and $f_c \propto U_j$. By comparing this estimated curve for the nozzle along with the reverser data, the orderly progression with velocity can be seen.

Effect of Jet Velocity on Noise

Maximum overall sound pressure level. - The effect of the isentropic nozzle jet velocity on the maximum overall sound pressure level at the 3.05-meter radius is illustrated in figure 10. The data shown are for the reverser at its optimum spacing with no offset and for the V-gutter reverser tested with a circular nozzle (ref. 1); data for the slot nozzle alone are also shown for comparison. The data for the two V-gutter reversers are in good agreement with each other and show a sixth-power dependence on velocity. Although screech was observed at the highest velocity (390 m/sec), there was no significant increase in OASPL above the sixth-power line faired through the lower velocity data. Subsonically, the slot nozzle follows an eighth-power dependence on velocity within the accuracy of the data, although a line faired through the two data points would yield an 8.5 power. For supersonic velocity, the combination of broad-band shock noise and screech tones yields noise levels about the same as with the reverser and well above an eighth-power extrapolation of the subsonic data.

Overall sound power level. - The variation of the effective overall sound-power level (OAPWL) with isentropic nozzle jet velocity is illustrated in figure 11. As mentioned earlier, the noise measured may, in principle, be a function of the angle of the microphone plane to the reverser, and the data are for one plane only; hence, these power levels are termed "effective." The data are shown for the same conditions as figure 10 for the reverser at its optimum spacing and no offset, for the V-gutter reverser of reference 1, and for the slot nozzle alone. Again, the data for the two reversers are in good agreement with each other and show a sixth-power velocity dependence and little effect of screech. The slot nozzle subsonically shows an eighth-power dependence on velocity, while shock noise and screech yield supersonic noise levels almost as high as for the reverser. The difference between levels for the slot nozzle with and without the reverser are about the same on the basis of OAPWL as on the basis of maximum OASPL.

Effect of Geometric Variables

The effect of geometric variables on the directivity of the overall sound pressure level and the spectra of sound pressure level and effective sound power level are presented in this section. The geometric variables investigated were the spacing between the nozzle and the reverser, the offset of the apex of the V-gutter from the nozzle-exit center plane, and the angle between the reverser-nozzle assembly and the microphone plane. Spacing and offset are defined in figure 6.

Spacing. - The effect of reverser-to-nozzle spacing on reverser noise at a jet velocity of 286 meters per second is illustrated in figure 12. Two spacings were tested: one was the optimum position, $X/D_h = -0.168$ (overlapped); and the other was $X/D_h = 0$, corresponding to the reverser leading edge being coplanar with the nozzle exit. The directivity plot (fig. 12(a)) shows that the data for $X/D_h = -0.168$ fall below those for $X/D_h = 0$ at all angles, but the difference is less than 1 dB except at angles of 20° and 40°. These minor differences are enough, however, to shift the angle for the maximum overall sound pressure level from 40° for $X/D_h = -0.168$ to 20° for $X/D_h = 0$. Figure 12(b) shows the SPL spectra for these two spacings at their maximum-OASPL angles, 40° for $X/D_h = -0.168$ and 20° for $X/D_h = 0$. The peak SPL occurs at slightly lower frequency for 0 spacing than for $X/D_h = -0.168$. The SPL data for $X/D_h = 0$ are higher from 200 to 12 500 hertz; but at the highest frequencies, the SPL for $X/D_h = -0.168$ is higher. The effective sound power level spectra in figure 12(c) show nearly the same effects. For the range of spacings tested, there was a slight increase in noise with increasing spacing, as was also observed for target reversers with the circular nozzle (ref. 1).

Offset. - The effect of offsetting the apex of the V-gutter from the nozzle exit plane is shown in figure 13 for jet velocities of 286 and about 360 meters per second. Data for no offset are compared with those for an offset of $Y_0 = 1.27$ centimeters. The directivity plots (fig. 13(a)) show that for all angles but 20°, there was less noise with the 1.27-centimeter offset. For 20°, the no-offset case gives more noise than the 1.27-centimeter offset at low velocity, but less at higher velocity. The maximum OASPL, at $\theta = 40^\circ$, is greater for the zero-offset configuration at both velocities. Slight differences in the SPL spectra at the angle of maximum OASPL can be seen in figure 13(b). In the vicinity of the peak, which occurs at high frequency, the sound pressure levels are higher with zero offset than with 1.27-centimeter offset; but at middle frequencies, the 1.27-centimeter offset sound pressure levels are higher. The differences are more evident at the lower velocity. In fact, at the lower velocity, the 1.27-centimeter data exhibit two peaks, or it might be interpreted as a single broad peak, both less in magnitude than the peak for zero offset. The effective sound power level spectra in fig-

ure 13(c) show essentially the same effects.

Orientation. - The effect of the orientation of the reverser and nozzle with respect to the microphone plane was checked by rotating the reverser and nozzle 90° with respect to the microphone plane. The results are shown in figure 14 for a nozzle jet velocity of approximately 360 meters per second, which corresponds to pressure ratios in the range of interest for the augmentor-wing slot stream. The effect of orientation on directivity is rather complicated, as illustrated in figure 14(a). With the reverser and nozzle vertical, the noise is directed more toward the sideline than for the horizontal position; and the angle of maximum OASPL is at 60°, compared with 40° for the horizontal orientation. The maximum OASPL is about the same for both cases. Figure 14(b) shows the SPL spectra at the angle of maximum OASPL; in the middle and high frequencies, the effects are not much greater than the data scatter. There is even less effect on the PWL spectra shown in figure 14(c).

For the nozzle alone, at approximately 285 meters per second velocity (fig. 15(a)), the effect of orientation on directivity is quite different than that with the reverser. (The comparison is made at lower velocity since shock and "screech" complicate the 360-m/sec data.) For the nozzle alone, the noise is directed more at the sideline in the horizontal position, for angles less than 120°; but the maximum OASPL occurs at both 140° and 160° vertically, compared with 160° horizontally. The SPL spectra for these three angle combinations are shown in figure 15(b). These spectral data are affected more strongly by the angle from the jet axis than by the orientation. As the angle shifts away from the jet axis, the peak of the SPL curve is flatter and occurs at higher frequency. Orientation has no significant effect on the power level spectra as shown in figure 15(c).

Sideline Shielding Experiments

A series of tests was conducted with plywood shields clamped to one side of the reverser support frame. These tests gave some information about the location of noise sources and also indicated a possible sideline noise reduction by shielding. These tests were all conducted with the reverser in its normal position and a nozzle jet velocity of about 357 meters per second. The 60° to 120° microphones were shielded, except for one run when the shield was moved forward 15.2 centimeters, shielding the 40° microphone but also exposing part of the reverser lip to the 120° microphone.

Figure 16 illustrates the effect of shielding on the sideline overall sound pressure level ($OASPL_S$). The presence of the shield just to the center plane of the nozzle and reverser caused a significant decrease in $OASPL_S$ for $60^{\circ} \leq \theta \leq 140^{\circ}$, with about a 4-dB

decrease at 80° through 120°. Raising the shield to 0.64 centimeter above the reverser upper lip further increased the attenuation significantly, giving about 6-dB total shielding effect at 80° and 100°. Further increases in shielding height gave little additional attenuation, with a little more than 7-dB shielding at 80° and 100° for the maximum shielding height of 15.9 centimeters above the upper reverser lip. Since the maximum $OASPL_S$ at 40° had not been affected by these changes, the shielding was moved forward 15.2 centimeters. This shielded smaller angles and removed the shielding from larger angles. About 3-dB attenuation was obtained at 40°. In addition, the attenuation at 60° through 80° was increased with little loss of attenuation at larger angles; a maximum attenuation of about 9 dB was obtained at $\theta = 80^{\circ}$. From these results it appears that shielding may have some potential for sideline noise reduction.

Some indication of the distribution of noise sources can be obtained from figure 17, which shows the SPL spectra at $\theta = 80^{\circ}$ for each of the shielding configurations. It can be seen that the effect of shielding is limited to frequencies of 500 hertz or higher, indicating that the predominant high-frequency noise sources are located in the region near the lip of the reverser. The low frequencies would then appear to be located away from the reverser in the region where the reversed jet mixes with the atmosphere; this matter is discussed further in the following section.

Sound Power Generated by Thrust Reversal

The thrust reverser had little effect on the low-frequency sound power level (fig. 9), and it appears that the dominant low-frequency noises were generated in the region where the reversed jet mixed with the atmosphere (fig. 17). Since the low-frequency PWL is about the same with the reverser as without it, it seems reasonable to isolate the sound power generated by thrust reversal (PWL_R) by antilogarithmically subtracting the nozzle-alone spectrum from the measured spectrum:

$$PWL_R = 10 \log\left(10^{PWL/10} - 10^{PWL_n/10}\right) \tag{3}$$

For the supersonic case, PWL_n is corrected for screech and broad-band shock noise as mentioned previously. The resulting PWL_R spectra are plotted in figure 18 for nozzle jet velocities of 190, 286, and 360 meters per second, with the normal reverser configuration. The trends with velocity are as might be expected: the levels and the peak-PWL_R frequency both increase with velocity. The data can then be normalized simply for the effects of velocity, as follows: 60 log U_j is subtracted from PWL_R because of the sixth-power law observed for overall power level, and the resulting normalized power level is plotted against frequency divided by velocity. Such a plot is shown in

figure 19 for the normal reverser configuration. It can be seen that this normalization scheme accounts for the effects of velocity quite well.

Sideline Perceived Noise Levels at Aircraft Scale

To obtain an estimate of the sideline perceived noise levels for wing-slot reversal on a 45 400-kilogram augmentor-wing-type STOL airplane, the experimental data for the normal reverser configuration have been scaled, as shown in figure 20. The data are scaled for a nozzle jet velocity of 362 meters per second, corresponding to a pressure ratio of 2.55, which is in the range of interest for the augmentor-wing slot. The slot area is scaled up to give 84 kilonewtons thrust, which would correspond to one wing of the airplane; it is assumed that the noise from only one of the wings would be heard. The data are shifted in frequency by the ratio of the small-scale to full-scale equivalent diameters, since such scaling is indicated by comparison of the present data with unpublished data for a larger-scale, higher-aspect-ratio model. Because of the shift of frequency by scaling, it was necessary to extrapolate the experimental data to higher frequencies; a dropoff of 2 dB per 1/3-octave band was assumed. It should be pointed out that the aspect ratio may also have an effect, but sufficient data are not yet available to establish such an effect. No account was made for any reflection from the aircraft, but the ground reflections of the experimental data were included. The data were corrected for atmospheric absorption according to reference 16; no correction was made for extra ground attenuation. The perceived noise level was then calculated for each angle according to reference 17. These calculated perceived noise levels are plotted against distance behind the airplane on the 152-meter sideline. The perceived noise levels are well above the 95-PNdB design goal for a considerable distance along the sideline. Shielding might provide some relief, but no calculation is made of the shielding benefit based on the data herein. The large change in slot aspect ratio from the experiment to the airplane would require a very large shield to get the same angular shielding. But perhaps a series of smaller, acoustically treated shields might give a significant sideline noise reduction. It is apparent from these results that noise considerations may well limit the use of wing-slot thrust reversal.

SUMMARY OF RESULTS

The results of this experimental investigation of the noise generated by a 2.26- by 11.43-centimeter slot nozzle with a V-gutter thrust reverser may be summarized as follows:

1. The V-gutter reverser generated more noise than the slot nozzle alone. Test results, when scaled up to conditions suitable for reversing the wing thrust of a 45 400-kilogram augmentor-wing-type airplane, showed that noise levels would be above the present design goal of 95 PNdB at the 152-meter sideline. This indicates that noise considerations may well limit the use of wing-slot thrust reversal.

2. The noise directivity patterns with the reverser were more uniform than those of the slot nozzle alone; both were more uniform than for a circular nozzle, but less uniform than a V-gutter reverser with the circular nozzle. The variation of overall sound pressure level (OASPL) with angle from the nozzle axis was no more than 8 dB in the plane of the nozzle long dimension and no more than 10 dB in the plane perpendicular to the nozzle long dimension. Maximum values of OASPL with the reverser occurred between the angles of 20° and 60° from the nozzle upstream axis, depending on the particular configuration. The uniformity of the noise directivity extended to the spectral distribution. The SPL distribution throughout the spectrum was similar in all directions.

3. The maximum OASPL and the effective overall power level both followed a sixth-power relation to isentropic nozzle jet velocity over the range of velocity tested, 190 to 360 meters per second. Data for the V-gutter reverser with the circular nozzle also showed good agreement with these relations.

4. The additional spectral sound power level due to thrust reversal (over and above that generated by the nozzle alone) was normalized as a function of velocity.

5. Preliminary experiments indicated that small shields might provide significant sideline noise reduction, but these tests were not definitive.

Lewis Research Center,
National Aeronautics and Space Administration,
Cleveland, Ohio, January 30, 1973,
501-24.

APPENDIX A

SYMBOLS

A_n	nozzle area, m^2
C1,C2,C3	first, second, and third frequency bands exhibiting ground-reflection cancellations, assuming a point source
D_e	equivalent circular diameter, $\sqrt{4A_n/\pi}$, m
D_h	hydraulic diameter, $4A_n$/(Nozzle perimeter), m
F_n	nozzle forward thrust, N
F_R	reverse thrust, N
f_c	1/3-Octave-band center frequency, Hz
H_n	nozzle slot height, m
H_R	larger of the two perpendicular distances from reverser to outer edge of nozzle lip, m
L	distance from nozzle exit plane to inside back of reverser, m
M_j	jet Mach number, dimensionless
$\dot{m}$	flow rate, kg/sec
$\dot{m}_n$	flow rate for nozzle alone, kg/sec
OAPWL	effective overall sound power level, dB re 10^{-13} W
OASPL	overall sound pressure level, dB re $20\mu N/m^2$
$OASPL_{max}$	maximum OASPL, dB re $20\mu N/m^2$
$OASPL_S$	overall sound pressure level on sideline, dB re $20\mu N/m^2$
P_a	ambient pressure, N/m^2 abs
P_n	nozzle inlet total pressure, N/m^2 abs
P_s	jet static pressure, N/m^2 abs
P_t	jet total pressure, N/m^2 abs
PNL	perceived noise level, PNdB
PWL	1/3-Octave-band effective sound power level, dB re 10^{-13} W
PWL_n	1/3-Octave-band effective sound power level due to nozzle alone, dB re 10^{-13} W

PWL_R	1/3-Octave-band effective sound power level due to thrust reversal, $10 \log\left(10^{PWL/10} - 10^{PWL_n/10}\right)$, dB re 10^{-13} W
R1,R2,R3	first, second, and third frequency bands exhibiting ground-reflection reinforcements, assuming a point source
SPL	1/3-Octave-band sound pressure level, dB re $20\mu N/m^2$
T_a	ambient temperature, K
T_n	nozzle inlet temperature, K
U_j	isentropic nozzle jet velocity, m/sec
U_{max}	maximum jet velocity at a given axial distance from nozzle, m
$\bar{W}_n$	average slot length, A_n/H_n, m
X	spacing between reverser exit plane and nozzle leading edge, m
x	distance downstream of nozzle exit plane, m
Y_0	offset of reverser apex from nozzle center plane, m
α	angle of reverser apex to horizontal, deg
θ	angle of microphone from nozzle upstream axis, deg
θ_{max}	angle of maximum OASPL, deg

APPENDIX B

EFFECTS OF SPACING ON FLOW AND THRUST REVERSAL

In order to verify that the noise tests were conducted at realistic reverser-to-nozzle spacings, the airflow rig shown in figure 3 was used to obtain data on flow and thrust-reversal efficiency, as well as the jet velocity survey data presented in appendix C. For the 2.26- by 11.43-centimeter slot nozzle alone, flow and thrust data were repeated with each velocity survey, thus yielding a large number of data points for essentially identical conditions. These data were averaged and are presented in figure 21, where flow rate and thrust are plotted against pressure ratio. Although these averaged data are in good agreement with the faired curves, it should be pointed out that the individual thrust data show a good deal of scatter (about ±27 N at each pressure ratio). This scatter is caused mainly by the fact that a 22 000-newton load cell was used. Consequently, the thrust data must be considered only qualitative.

The effects of spacing on flow rate and thrust reversal for the 2.26- by 11.43-centimeter slot nozzle with the V-gutter thrust reverser are illustrated in figure 22. The flow rate divided by the flow rate for the nozzle alone at the same pressure ratio (from fig. 21(a)) is plotted against the reverser-to-nozzle spacing ratio in figure 22(a). Similarly, the reverse thrust divided by the forward thrust for the nozzle alone (from fig. 21(b)) is plotted against this spacing ratio in figure 22(b). The effect of spacing on flow ratio increases with decreasing pressure ratio; in fact, for $P_n/P_a = 3.0$, there is essentially no effect at all over the range tested. It appears that full flow is obtained for $X/D_h \geq -0.32$ at pressure ratios of 2.0 or more, and for $X/D_h \geq -0.16$ for pressure ratios less than 2.0. The thrust data show too much scatter (there was no repetition to average the data) for other than qualitative conclusions to be drawn. At $X/D_h = -0.16$, where most of the acoustic data were obtained, thrust-reversal efficiencies are of the order of 40 percent; and at $X/D_h = +0.18$ the efficiency is in the 50-percent range. However, increasing the spacing also increased the noise for the acoustic data reported herein.

APPENDIX C

SLOT-NOZZLE JET VELOCITY SURVEYS

Slot-nozzle jet velocity surveys are presented in this appendix, since such data may aid in understanding the nozzle noise-generating mechanisms and also because the rate of velocity decay itself is important for externally-blown-flap configurations (ref. 18). The x-y-y' plotter produced plots of total pressure against distance from the nozzle centerline and also a similar plot of the static pressure 1.27 centimeters further downstream. Such plots were obtained for the nozzle long dimension and the probe travel both horizontal, for nozzle pressure ratios from 1.25 to 3.00 (fig. 23). Figure 24 shows similar plots for the nozzle long dimension vertical and the probe travel horizontal. In each of these figures the distance of the total-pressure probe downstream of the nozzle exit plane was 0.64 centimeter in part (a), 1.27 centimeters in part (b), 2.54 centimeters in part (c), 5.08 centimeters in part (d), 10.16 centimeters in part (e), 20.3 centimeters in part (f), and 36.8 centimeters in part (g). It may be observed that for pressure ratios low enough not to have strong shocks, the maximum jet velocity was essentially unchanged within the range of distance where the thrust reverser was located.

When these pressure profiles are used, the local maximum jet velocity can be computed from reference 19. In some cases the static pressure must be estimated by interpolation to match the distance of the total pressure. For the relatively low supersonic Mach numbers involved, no correction was made to the total-pressure readings for bow shocks; this might cause as much as a 2-percent error at 2.5 pressure ratio and 6 percent at 3.0. Maximum jet velocities are compared with the correlation of reference 18 in figure 25; the subsonic data are shown in figure 25(a), and the supersonic data are shown in figure 25(b). The maximum local velocity is divided by the calculated isentropic jet velocity and plotted against the nondimensional distance parameter $x/D_e\sqrt{1 + M_j}$. The subsonic and low supersonic data agree reasonably well with the correlation of reference 18; but the 3.0-pressure-ratio data do show considerable disagreement, perhaps because of shock effects. This effect is certainly greater than any bow-shock errors in the probe readings.

REFERENCES

1. Gutierrez, Orlando A.; and Stone, James R.: Preliminary Experiments on the Noise Generated by Target-Type Thrust Reverser Models. NASA TM X-2553, 1972.

2. Stone, J. R.; and Gutierrez, O. A.: Noise Generated by STOL Core-Jet Thrust Reversers. Paper 72-791, AIAA, Aug. 1972.

3. Reshotko, Meyer; Olsen, William A.; and Dorsch, Robert G.: Preliminary Noise Tests of the Engine-Over-the-Wing Concept. I: 30°-60° Flap Position. NASA TM X-68032, 1972.

4. Reshotko, Meyer; Olsen, William A.; and Dorsch, Robert G.: Preliminary Noise Tests of the Engine-Over-the-Wing Concept. II: 10°-20° Flap Position. NASA TM X-68104, 1972.

5. Olsen, William A.; Dorsch, Robert G.; and Miles, Jeffrey H.: Noise Produced by a Small-Scale, Externally Blown Flap. NASA TN D-6636, 1972.

6. Dorsch, R. G.; Kreim, W. J.; and Olsen, W. A.: Externally-Blown-Flap Noise. Paper 72-129, AIAA, Jan. 1972.

7. Dorsch, R. G.; Krejsa, E. A.; and Olsen, W. A.: Blown Flap Noise Research. Paper 71-745, AIAA, June 1971.

8. Povolny, John H.; Steffen, Fred W.; and McArdle, Jack G.: Summary of Scale-Model Thrust-Reverser Investigation. NACA Rept. 1314, 1957.

9. Ashwood, P. F.: The Preliminary Testing of an Aerodynamic Design of Thrust Spoiler. Memo. M. 138, National Gas Turbine Establishment, England, Oct. 1951.

10. Poland, Dyckman T.: The Aerodynamics of Thrust Reversers for High Bypass Turbofans. Paper 67-418, AIAA, July 1967.

11. Tolhurst, William H., Jr.; Hickey, David H.; and Aoyagi, Kiyoshi: Large-Scale Wind-Tunnel Tests of Exhaust Ingestion Due to Thrust Reversal on a Four-Engine Jet Transport During Ground Roll. NASA TN D-686, 1961.

12. Kohl, Robert C.; and Algaranti, Joseph S.: Investigation of a Full-Scale, Cascade-Type Thrust Reverser. NACA TN 3975, 1957.

13. Falarski, Michael D.; and Mort, Kenneth W.: Full-Scale Wind-Tunnel Investigation of a Target-Type Thrust Reverser on the A-37B Airplane. NASA TM X-1985, 1970.

14. Kohl, Robert C.: Performance and Operational Studies of a Full-Scale Jet-Engine Thrust Reverser. NACA TN 3665, 1956.

15. Huff, Ronald G.; and Groesbeck, Donald E.: Splitting Supersonic Nozzle Flow into Separate Jets by Overexpansion into a Multilobed Divergent Nozzle. NASA TN D-6667, 1972.

16. Anon.: Noise Standards: Aircraft Type Certification. Federal Aviation Regulations, Vol. III, Part 36, 1969.

17. Anon.: Definitions and Procedures for Computing the Perceived Noise Level of Aircraft Noise. Aerospace Recommended Practice 865A, SAE, Aug. 15, 1969.

18. von Glahn, U. H.; Groesbeck, D. E.; and Huff, R. G.: Peak Axial-Velocity Decay With Single- and Multi-Element Nozzles. Paper 72-48, AIAA, Jan. 1972.

19. Ames Research Staff: Equations, Tables, and Charts for Compressible Flow. NACA Rept. 1135, 1953.

TABLE I. - SUMMARY OFACOUSTIC DATA

Run	Spacing ratio, X/D_h	Angle to horizontal, α, deg	Offset, Y_0, cm	Pressure ratio, P_n/P_a	Effective overall power level, OAPWL, dB re 10^{-13} W	Frequency of maximum PWL, kHz	Maximum overall sound pressure level, $OASPL_{max}$, dB re 20 $\mu N/m^2$	Angle of maximum OASPL, θ_{max}, deg	Frequency of maximum SPL at θ_{max}, kHz
				Slot nozzle and V-gutter reverser					
[a]1	-0.168	0	0	1.73	144	8	120	40	8
[a]2	-.168			2.55	149	10	126	40	10
[a]3	0			1.73	144	5	121	20	6.3
4	-.168			2.55	150	12.5	127	40	8
[b]5				3.03	[b]152	[b]8	[b]129	40	[b]8
6				1.26	134	4	110	20	10
7			1.27	1.73	142	8 to 10	119	20 40	2.5 6.3, 10
8			1.27	2.55	150	10 to 12.5	126	20 40	8 10
9		90	0	2.55	150	8	126	60	8
10		0	0	2.54	150	12.5	127	40	12.5
				Slot nozzle alone					
[b]16	------	0	----	2.54	[b]148	[b]8	[b]126	140	[b]4
17	------		----	1.74	132	3.15	110	160	1
18	------		----	1.25	116		92	160	1
19	------	90	----	1.7	132		110	140 160	3.15 1
				Slot nozzle and V-gutter reverser with shields					
11	-0.168	0	0	2.54	Shield at V		127	40	10
12					Shield 0.64 cm above V				12.5
13					Shield 8.26 cm above V				12.5
14					Shield 15.9 cm above V				10
15					Shield 15.9 cm above V and forward 15.2 cm		124		10 to 12.5

[a]No acoustic backing.
[b]Screech.

TABLE II. - DETAILED ACOUSTIC DATA

Run 1 - No acoustic backing	
Spacing ratio, X/D_h, -0.168	Normal horizontal position
Pressure ratio, P_n/P_a, 1.73	Nozzle jet velocity, U_j, 286 m/sec
Nozzle inlet temperature, T_n, 278 K	Ambient temperature, T_a, 270 K
Ambient pressure, P_a, 99.2 kN/m^2 abs	Relative humidity, 60 percent

1/3-Octave-band center frequency, f_c, Hz	Angle from nozzle axis, θ, deg									Power level, PWL, dB re 10^{-13} W
	20	40	60	80	100	120	140	160	180	
	Sound pressure level on 3.05-m radius, SPL, dB re 20 μN/m^2									
50	68.5	70.0	68.7	68.5	-----	77.7	82.0	81.2	77.2	-----
63	71.5	71.2	73.0	70.5	73.5	77.0	76.0	82.2	80.5	-----
80	75.2	74.5	74.5	73.5	73.5	78.7	85.0	83.7	80.7	-----
100	75.5	73.5	73.5	72.8	73.2	78.5	85.5	77.2	80.0	-----
125	80.0	80.8	78.7	78.0	80.2	80.3	84.5	82.5	79.5	-----
160	78.2	78.2	78.2	76.8	78.3	79.5	78.5	76.7	74.7	-----
200	80.3	79.3	78.7	78.2	78.7	82.7	78.0	77.5	77.7	-----
250	82.2	82.0	81.2	80.7	82.2	87.3	82.5	81.5	81.7	110.1
315	81.8	81.8	80.8	81.2	82.7	87.8	83.8	83.0	83.0	110.6
400	83.4	83.2	81.9	81.7	83.2	84.5	85.0	81.8	82.0	110.3
500	86.9	87.0	85.7	85.5	86.9	87.0	86.2	84.9	84.9	113.4
630	88.2	87.9	85.5	86.0	87.2	87.7	86.5	86.4	86.4	114.1
800	92.0	91.5	88.9	89.9	90.4	90.5	89.9	89.0	90.0	117.5
1 000	95.4	93.1	92.7	92.9	93.1	94.1	93.1	93.2	94.4	120.7
1 250	96.7	96.9	94.9	94.9	94.9	96.1	96.7	95.4	95.6	123.0
1 600	98.2	98.2	97.1	96.7	96.9	97.2	97.1	97.6	96.6	124.5
2 000	100.4	99.8	99.8	99.3	98.8	98.3	98.9	98.8	100.1	126.5
2 500	102.8	102.5	101.6	100.3	99.1	99.1	98.8	99.8	102.5	128.0
3 150	107.7	107.0	106.7	103.7	102.2	103.0	101.0	103.7	105.0	132.1
4 000	109.9	109.5	108.7	105.9	103.7	103.9	101.2	104.0	105.2	133.9
5 000	110.9	110.4	108.4	105.6	103.9	103.3	101.1	103.8	104.3	134.2
6 300	110.7	111.0	109.5	105.7	104.3	104.0	102.0	104.0	104.3	134.6
8 000	110.7	111.4	109.9	106.7	103.7	104.7	102.6	104.7	105.1	135.0
10 000	110.0	110.7	109.8	105.3	102.5	104.0	102.3	103.3	103.3	134.3
12 500	108.8	110.3	108.1	104.5	101.5	103.1	102.6	102.0	103.1	133.4
16 000	107.0	109.1	106.5	102.5	100.5	101.3	102.3	100.3	101.5	131.9
20 000	105.4	108.4	105.4	101.9	99.9	100.2	101.0	98.4	99.0	130.8
Overall	119.2	119.7	118.2	114.9	112.9	113.4	112.2	113.3	114.1	143.5

TABLE II. - Continued. DETAILED ACOUSTIC DATA

Run 2 - No acoustic backing	
Spacing ratio, X/D_h, -0.168	Normal horizontal position
Pressure ratio, P_n/P_a, 2.55	Nozzle jet velocity, U_j, 362 m/sec
Nozzle inlet temperature, T_n, 278 K	Ambient temperature, T_a, 270 K
Ambient pressure, P_a, 99.2 kN/m^2 abs	Relative humidity, 60 percent

1/3-Octave-band center frequency, f_c, Hz	Angle from nozzle axis, θ, deg									Power level, PWL, dB re 10^{-13} W
	20	40	60	80	100	120	140	160	180	
	Sound pressure level on 3.05-m radius, SPL, dB re 20 $\mu N/m^2$									
50	75.8	80.3	78.0	73.5	73.5	73.3	71.7	73.5	72.7	-----
63	78.5	81.7	78.5	74.7	76.3	76.7	75.7	76.5	75.2	-----
80	80.0	82.5	78.5	77.0	77.3	77.0	77.0	77.7	77.8	-----
100	80.8	83.3	78.5	77.5	78.5	77.5	77.7	76.7	78.2	-----
125	83.5	86.0	81.7	80.7	80.7	80.8	78.5	79.5	80.8	-----
160	86.5	86.7	82.5	80.3	80.2	80.0	79.5	79.8	79.3	-----
200	89.2	88.2	85.7	84.3	84.8	85.0	84.7	85.3	85.8	-----
250	91.3	90.3	88.0	87.7	88.8	89.0	89.8	90.0	90.2	116.7
315	91.3	91.0	88.2	88.3	88.7	89.8	90.8	91.3	91.7	117.4
400	92.5	92.0	89.0	88.7	89.0	89.2	89.5	89.9	90.5	117.4
500	95.5	94.7	92.7	93.4	94.2	93.7	92.7	92.7	93.2	120.9
630	95.9	95.2	92.7	93.2	93.5	93.0	93.5	94.2	94.7	121.2
800	99.2	98.4	96.5	96.7	96.9	96.9	96.9	97.0	97.4	124.6
1 000	102.7	100.4	99.7	99.7	99.2	100.6	100.1	100.2	100.4	127.6
1 250	104.2	103.7	102.1	100.9	100.4	101.1	101.4	100.7	100.7	129.1
1 600	106.2	105.2	103.1	103.1	102.2	101.4	101.7	101.1	100.9	130.4
2 000	107.3	106.3	105.9	105.1	104.1	102.6	102.9	101.8	102.9	131.9
2 500	108.5	108.6	107.3	105.8	105.0	103.6	103.1	102.1	104.1	133.2
3 150	112.2	111.5	111.5	109.2	107.5	106.3	104.3	104.0	105.5	136.3
4 000	111.5	114.0	112.7	111.2	109.0	107.0	104.7	105.2	105.9	137.5
5 000	113.3	116.6	114.1	111.6	110.1	108.1	105.9	106.8	107.1	139.2
6 300	113.0	116.8	115.3	111.8	110.2	109.0	107.0	108.3	107.2	139.6
8 000	113.4	118.2	116.2	113.1	110.1	110.1	108.2	109.2	108.4	140.6
10 000	113.5	118.5	116.5	112.7	110.2	109.5	108.8	109.3	109.0	140.8
12 500	112.3	117.3	115.3	112.0	109.8	109.1	110.1	109.6	110.6	140.0
16 000	112.6	116.6	115.6	111.8	109.8	109.5	111.5	109.8	111.3	140.0
20 000	110.9	115.2	114.5	111.4	109.7	109.2	110.9	108.7	109.9	139.0
Overall	122.7	126.3	124.7	121.7	119.7	118.9	118.7	118.4	118.9	149.3

TABLE II. - Continued. DETAILED ACOUSTIC DATA

Run 3 - No acoustic backing										
Spacing ratio, X/D_h, 0						Normal horizontal position				
Pressure ratio, P_n/P_a, 1.73						Nozzle jet velocity, U_j, 286 m/sec				
Nozzle inlet temperature, T_n, 278 K						Ambient temperature, T_a, 270 K				
Ambient pressure, P_a, 99.2 kN/m^2 abs						Relative humidity, 60 percent				
1/3-Octave-band center frequency, f_c, Hz	Angle from nozzle axis, θ, deg									Power level, PWL, dB re 10^{-13} W
	20	40	60	80	100	120	140	160	180	
	Sound pressure level on 3.05-m radius, SPL, dB re 20 μN/m^2									
50	70.2	70.0	70.7	70.2	71.2	71.0	69.0	70.0	-----	-----
63	73.2	72.0	72.0	72.5	72.5	72.2	72.0	73.2	72.7	-----
80	75.7	76.5	75.5	74.8	74.7	73.7	73.5	76.2	75.7	-----
100	75.0	74.7	73.0	74.0	73.3	73.3	73.0	74.5	76.0	-----
125	79.5	80.7	78.5	77.8	78.8	78.8	76.0	77.2	79.3	-----
160	78.2	77.5	78.0	76.5	76.3	76.0	74.5	75.7	75.8	-----
200	80.2	79.7	79.3	78.3	78.5	78.2	77.2	77.7	78.0	-----
250	82.3	81.8	81.8	80.3	81.2	81.5	82.0	81.2	80.3	108.6
315	82.3	81.8	81.7	80.3	81.0	81.8	82.0	82.0	81.7	108.8
400	83.9	83.0	82.5	81.7	81.9	81.5	81.5	81.0	81.0	109.3
500	87.5	86.9	85.2	85.4	86.7	86.7	85.9	84.9	84.7	113.3
630	89.0	88.2	86.2	86.5	87.7	87.7	86.2	86.2	86.7	114.5
800	93.4	92.5	89.9	90.9	91.4	91.0	90.4	89.9	91.0	118.5
1 000	96.4	93.7	93.7	93.2	93.2	94.4	93.6	93.6	95.1	121.3
1 250	97.2	97.6	95.6	95.1	94.9	95.7	96.4	95.4	96.6	123.3
1 600	98.9	99.2	97.1	96.4	96.7	97.1	97.4	97.2	97.2	124.8
2 000	101.4	101.1	100.6	98.8	98.8	99.6	99.1	99.8	101.3	127.2
2 500	104.6	104.1	102.5	101.1	100.1	100.3	99.8	101.3	103.6	129.4
3 150	108.0	108.7	107.2	104.0	102.7	103.0	101.3	104.2	104.8	132.7
4 000	110.7	111.0	109.4	105.2	102.9	103.2	101.4	104.2	105.9	134.5
5 000	112.9	112.8	110.3	105.9	104.6	103.8	101.9	103.4	105.6	135.9
6 300	113.2	112.2	109.8	106.2	104.7	104.2	102.3	104.3	104.3	135.8
8 000	112.2	111.6	109.9	106.6	104.2	104.7	103.1	105.2	105.2	135.5
10 000	111.5	111.5	110.2	106.2	103.5	104.0	102.3	103.3	103.5	135.1
12 500	111.0	110.5	108.1	104.5	102.0	103.1	102.5	101.8	103.1	134.0
16 000	107.8	108.5	106.6	103.0	101.3	101.5	102.1	99.8	101.3	132.0
20 000	106.0	107.0	104.9	101.9	100.2	100.0	100.4	97.7	98.9	130.3
Overall	120.7	120.5	118.6	115.1	113.3	113.5	112.4	113.5	114.5	144.2

TABLE II. - Continued. DETAILED ACOUSTIC DATA

Run 4										
Spacing ratio, X/D_h, -0.168					Normal horizontal position					
Pressure ratio, P_n/P_a, 2.55					Nozzle jet velocity, U_j, 363 m/sec					
Nozzle inlet temperature, T_n, 279 K					Ambient temperature, T_a, 278 K					
Ambient pressure, P_a, 98.2 kN/m^2 abs					Relative humidity, 52 percent					
1/3-Octave-band center frequency, f_c, Hz	Angle from nozzle axis, θ, deg									Power level, PWL, dB re 10^{-13} W
	20	40	60	80	100	120	140	160	180	
	Sound pressure level on 3.05-m radius, SPL, dB re 20 μN/m^2									
50	78.0	80.7	78.0	73.3	73.0	72.2	71.3	73.0	73.3	-----
63	79.0	82.2	78.5	75.5	75.2	74.7	75.3	76.0	75.3	-----
80	80.8	83.2	79.0	77.0	77.2	76.2	76.2	78.5	77.2	-----
100	81.5	83.7	79.5	78.3	78.3	77.5	77.3	78.0	78.0	-----
125	83.0	84.8	82.7	80.7	79.2	78.2	78.8	80.2	81.0	-----
160	84.8	86.5	82.0	80.5	79.8	80.0	79.8	79.7	79.5	-----
200	88.0	88.3	85.0	84.0	84.2	84.7	85.3	85.5	85.7	-----
250	91.5	90.3	88.2	88.0	88.5	88.8	89.5	89.8	89.8	116.7
315	91.0	91.0	88.5	88.2	88.3	88.5	90.0	90.5	90.7	116.8
400	91.0	91.2	88.4	88.0	87.9	88.0	88.2	89.0	89.2	116.4
500	93.9	93.7	91.4	92.5	92.9	91.9	91.5	91.7	91.7	119.9
630	94.9	94.4	91.7	92.5	93.0	92.9	93.0	93.9	94.4	120.6
800	99.7	97.7	95.0	96.5	96.5	96.0	96.2	96.4	96.5	124.2
1 000	103.4	100.2	98.9	99.0	98.9	99.4	99.2	99.7	99.4	127.2
1 250	105.1	103.6	100.7	99.7	99.6	100.2	100.4	99.6	99.1	128.6
1 600	106.7	104.9	102.6	101.9	101.2	100.6	100.6	100.1	99.1	130.0
2 000	108.8	107.1	105.3	104.1	103.3	101.9	101.4	100.4	101.1	132.0
2 500	109.4	109.1	107.1	106.1	104.9	102.9	102.1	101.4	102.3	133.6
3 150	113.6	112.8	110.8	109.0	107.8	105.6	103.6	103.6	104.1	137.0
4 000	113.5	114.3	112.5	110.7	108.5	106.3	104.0	104.7	104.8	138.1
5 000	114.7	117.1	113.9	111.7	109.6	106.7	105.4	105.7	106.1	139.7
6 300	115.1	118.0	115.8	112.3	109.5	108.1	106.5	106.6	106.8	140.7
8 000	116.4	119.2	116.7	113.2	111.4	109.9	107.9	107.9	107.7	141.9
10 000	114.3	118.3	115.6	111.8	109.8	108.5	107.5	106.8	107.5	140.7
12 500	113.6	118.4	115.6	112.2	109.9	108.2	108.4	106.9	108.6	140.8
16 000	112.4	116.7	114.6	111.4	109.9	108.4	108.9	106.4	109.2	139.8
20 000	112.7	116.7	114.6	110.7	109.2	108.2	108.7	106.6	109.4	139.7
Overall	124.2	126.9	124.5	121.5	119.6	118.0	117.3	116.5	117.5	149.9

TABLE II. - Continued. DETAILED ACOUSTIC DATA

Run 5										
Spacing ratio, X/D_h, -0.168					Normal horizontal position					
Pressure ratio, P_n/P_a, 3.03					Nozzle jet velocity, U_j, 390 m/sec					
Nozzle inlet temperature, T_n, 279 K					Ambient temperature, T_a, 278 K					
Ambient pressure, P_a, 98.2 kN/m^2 abs					Relative humidity, 52 percent					
1/3-Octave-band center frequency, f_c, Hz	Angle from nozzle axis, θ, deg									Power level, PWL, dB re 10^{-13} W
	20	40	60	80	100	120	140	160	180	
	Sound pressure level on 3.05-m radius, SPL, dB re 20 $\mu N/m^2$									
50	81.2	88.5	80.0	76.2	76.0	74.8	73.7	74.5	75.5	-----
63	82.7	89.0	82.0	78.7	78.7	78.3	79.5	79.2	77.7	-----
80	84.2	90.0	81.8	80.2	80.7	80.0	79.7	80.5	80.3	-----
100	84.7	90.3	83.8	82.7	82.5	81.3	81.5	80.7	80.8	-----
125	85.7	91.8	84.7	82.5	81.8	81.2	81.7	81.7	82.7	-----
160	88.7	92.7	85.5	82.7	82.2	82.0	81.8	81.2	81.0	-----
200	91.5	93.7	87.5	85.8	86.0	86.3	87.2	87.7	87.8	-----
250	93.3	94.0	90.5	89.5	89.8	91.0	92.3	92.7	92.7	119.0
315	92.7	94.7	90.7	90.0	90.7	91.2	92.0	92.5	92.8	119.2
400	92.7	94.7	91.0	89.7	89.5	89.0	89.7	90.4	90.4	118.5
500	95.9	96.9	94.2	94.0	94.2	94.0	94.0	94.0	93.7	122.1
630	96.7	98.0	94.7	94.7	95.2	95.5	96.0	95.7	96.0	123.3
800	102.4	101.9	99.0	99.0	99.9	100.4	100.4	100.2	99.5	127.8
1 000	105.9	104.4	103.0	102.4	103.7	104.9	104.2	104.0	103.5	131.5
1 250	107.7	106.2	104.4	104.4	105.4	106.2	104.7	103.9	103.7	132.9
1 600	109.2	108.4	104.9	104.9	104.2	104.4	103.9	102.6	102.1	133.0
2 000	111.8	109.6	107.9	107.1	106.4	105.3	104.8	103.4	103.9	134.9
2 500	112.1	111.8	110.4	108.8	107.4	105.9	105.4	103.8	104.6	136.4
3 150	115.0	114.8	113.6	111.1	109.5	107.6	106.0	106.3	106.3	139.1
4 000	114.3	115.8	114.5	112.2	110.5	108.0	106.7	107.3	107.3	139.8
5 000	115.2	117.2	115.7	112.9	111.1	108.2	107.1	108.1	107.9	140.8
6 300	116.6	118.5	117.0	113.3	111.1	109.8	108.1	108.8	109.3	141.8
8 000	121.5	124.0	122.5	118.7	114.7	112.2	111.2	111.7	111.4	146.9
10 000	117.6	119.3	118.0	114.3	112.6	111.1	110.3	110.5	110.8	142.9
12 500	116.1	117.9	116.7	113.9	112.6	111.1	111.1	110.4	112.1	142.0
16 000	115.6	117.6	117.1	113.7	112.7	111.7	112.4	109.9	112.9	142.1
20 000	114.1	116.4	116.4	113.6	111.9	111.2	111.4	109.6	112.2	141.3
Overall	126.9	128.7	127.4	124.2	122.2	120.7	120.2	119.7	120.6	152.4

TABLE II. - Continued. DETAILED ACOUSTIC DATA

Run 6	
Spacing ratio, X/D_h, -0.168	Normal horizontal position
Pressure ratio, P_n/P_a, 1.26	Nozzle jet velocity, U_j, 190 m/sec
Nozzle inlet temperature, T_n, 278 K	Ambient temperature, T_a, 278 K
Ambient pressure, P_a, 98.2 kN/m^2 abs	Relative humidity, 52 percent

1/3-Octave-band center frequency, f_c, Hz	Angle from nozzle axis, θ, deg									Power level, PWL, dB re 10^{-13} W
	20	40	60	80	100	120	140	160	180	
	Sound pressure level on 3.05-m radius, SPL, dB re 20 $\mu N/m^2$									
50	69.3	69.3	69.8	68.7	67.3	66.5	66.0	68.8	71.7	-----
63	72.2	72.8	72.2	72.3	71.7	71.7	72.2	72.7	72.3	-----
80	73.3	72.3	72.8	75.5	73.3	73.3	73.7	75.2	74.3	-----
100	71.5	71.8	71.2	72.8	74.2	74.0	73.0	73.0	74.5	-----
125	77.0	77.5	77.0	77.7	77.3	73.8	75.8	75.2	78.2	-----
160	69.7	70.0	69.7	70.8	70.3	70.7	70.8	71.0	71.5	-----
200	70.8	70.5	70.5	70.2	70.5	70.7	71.0	70.5	70.7	-----
250	75.5	75.8	74.7	79.0	75.7	77.5	77.3	76.2	74.2	104.3
315	72.7	72.8	71.8	73.3	72.8	73.2	73.2	73.0	72.8	100.4
400	73.2	73.9	72.5	72.4	73.0	72.5	72.0	72.4	72.2	100.2
500	78.0	78.0	76.7	76.5	77.4	76.9	77.0	77.4	77.9	104.6
630	79.5	79.5	78.2	77.9	78.2	78.2	78.5	79.7	80.2	106.1
800	85.5	84.4	82.4	81.4	82.5	83.0	85.0	85.9	86.5	111.0
1 000	89.0	87.9	87.7	84.7	86.4	88.4	89.4	90.5	91.0	115.4
1 250	90.1	93.7	90.2	88.7	88.6	91.2	93.7	92.7	92.4	118.7
1 600	92.4	94.2	91.4	90.9	90.6	92.6	95.4	94.6	93.7	120.2
2 000	95.1	95.3	93.4	92.6	93.8	95.3	95.1	96.4	97.6	122.0
2 500	98.6	98.3	96.9	94.4	94.4	94.4	95.4	96.6	98.6	123.6
3 150	100.1	99.8	97.8	95.6	95.0	94.1	93.1	95.3	96.1	124.2
4 000	100.8	102.0	99.0	96.8	95.2	94.2	92.2	94.5	95.2	125.2
5 000	100.7	100.4	98.4	95.2	92.9	92.1	90.1	92.2	94.1	124.0
6 300	100.5	100.0	98.8	94.0	91.5	91.1	89.6	91.3	93.8	123.6
8 000	100.0	98.9	96.4	93.2	90.5	91.0	88.5	90.2	92.7	122.4
10 000	101.8	100.8	99.1	95.3	91.6	90.3	88.8	89.3	91.3	124.2
12 500	99.2	98.2	95.9	92.9	89.1	88.1	87.4	86.1	88.9	121.6
16 000	97.4	95.7	93.9	91.2	87.9	85.7	85.9	83.1	86.9	119.5
20 000	95.6	94.2	91.4	89.2	85.7	83.9	83.7	81.4	84.9	117.6
Overall	110.1	109.8	107.7	104.9	103.4	103.4	103.5	104.4	105.6	133.9

TABLE II. - Continued. DETAILED ACOUSTIC DATA

Run 7										
Spacing ratio, X/D_h, -0.168					Horizontal; V apex 1.27 cm below nozzle center					
Pressure ratio, P_n/P_a, 1.73					Nozzle jet velocity, U_j, 286 m/sec					
Nozzle inlet temperature, T_n, 279 K					Ambient temperature, T_a, 278 K					
Ambient pressure, P_a, 98.2 kN/m^2 abs					Relative humidity, 52 percent					
1/3-Octave-band center frequency, f_c, Hz	Angle from nozzle axis, θ, deg									Power level, PWL, dB re 10^{-13} W
	20	40	60	80	100	120	140	160	180	
	Sound pressure level on 3.05-m radius, SPL, dB re 20 $\mu N/m^2$									
50	68.8	68.0	69.7	66.7	-----	66.0	66.5	69.7	69.2	-----
63	71.7	71.5	71.7	71.0	70.2	71.7	71.5	71.5	72.0	-----
80	74.0	73.3	74.7	77.2	77.0	73.5	74.2	76.8	76.7	-----
100	73.2	74.5	74.5	74.5	77.0	75.2	75.5	74.8	75.3	-----
125	78.2	78.8	78.7	79.7	79.2	75.2	77.5	76.7	78.2	-----
160	73.5	73.8	76.0	76.2	74.0	73.5	73.5	73.8	73.5	-----
200	75.7	75.2	76.5	76.0	76.2	75.7	74.2	74.8	74.7	-----
250	79.5	80.5	79.8	81.7	80.3	80.3	78.5	79.8	77.8	107.8
315	80.3	79.5	78.8	78.0	78.0	77.5	77.5	77.7	78.0	105.9
400	82.7	82.4	82.0	81.4	80.7	80.0	79.7	79.4	79.9	108.6
500	87.2	86.9	85.7	84.7	84.7	83.7	83.5	83.7	84.4	112.6
630	89.0	88.2	86.0	85.7	86.2	85.9	85.7	86.5	87.2	114.0
800	94.4	93.0	90.0	89.2	89.4	89.2	90.0	91.0	91.5	118.2
1 000	98.2	95.9	95.5	93.0	92.5	93.2	94.2	96.2	97.0	122.2
1 250	99.7	99.9	97.7	94.2	93.4	97.1	97.1	97.2	97.2	124.6
1 600	100.9	100.1	99.7	98.1	95.1	97.1	99.2	98.2	98.1	126.1
2 000	105.3	105.9	102.8	100.8	97.8	98.6	100.3	102.1	103.1	129.5
2 500	109.8	108.8	105.4	101.8	100.1	100.3	102.3	103.4	105.9	132.2
3 150	109.6	109.1	105.1	102.1	100.5	99.0	99.1	101.3	104.6	132.0
4 000	109.2	108.2	105.3	102.8	100.8	98.5	98.7	100.0	103.0	131.7
5 000	107.6	108.2	105.9	102.7	100.2	98.2	98.2	99.6	100.7	131.4
6 300	108.1	109.3	106.3	103.3	100.6	99.6	98.6	99.6	100.6	132.1
8 000	108.9	109.0	106.4	103.4	101.7	99.7	99.7	100.5	100.5	132.3
10 000	108.3	109.3	106.8	103.6	101.6	99.3	99.5	99.5	99.8	132.3
12 500	108.2	108.9	105.9	103.7	101.7	99.7	100.4	98.7	100.2	132.1
16 000	106.7	107.6	105.1	102.4	100.7	98.9	99.4	96.7	99.6	130.9
20 000	105.1	106.4	103.9	101.9	99.6	97.9	97.7	95.4	97.7	129.7
Overall	118.7	118.9	116.1	113.4	111.3	110.2	110.7	111.3	113.0	142.2

TABLE II - Continued. DETAILED ACOUSTIC DATA

Run 8										
Spacing ratio, X/D_h, -0.168					Horizontal; V apex 1.27 cm below nozzle center					
Pressure ratio, P_n/P_a, 2.55					Nozzle jet velocity, U_j, 363 m/sec					
Nozzle inlet temperature, T_n, 279 K					Ambient temperature, T_a, 278 K					
Ambient pressure, P_a, 98.2 kN/m^2 abs					Relative humidity, 52 percent					
1/3-Octave-band center frequency, f_c, Hz	Angle from nozzle axis, θ, deg									Power level, PWL, dB re 10^{-13} W
	20	40	60	80	100	120	140	160	180	
	Sound pressure level on 3.05-m radius, SPL, dB re 20 $\mu N/m^2$									
50	78.0	78.2	78.0	69.3	69.0	68.2	68.8	70.5	71.2	-----
63	78.0	79.3	78.0	71.8	71.5	72.8	73.0	72.3	72.8	-----
80	78.7	79.8	78.3	75.0	74.7	75.0	75.2	77.2	76.2	-----
100	79.0	80.3	78.0	75.0	76.2	75.8	76.2	75.3	76.2	-----
125	82.3	82.5	80.2	78.8	79.0	76.0	78.7	77.5	79.7	-----
160	84.3	83.3	78.8	77.7	77.3	76.8	76.8	77.0	76.3	-----
200	86.7	86.0	83.0	81.8	81.5	81.2	81.2	81.3	81.3	-----
250	88.7	88.3	86.8	86.0	85.3	86.3	86.3	86.3	86.2	114.2
315	89.0	89.0	86.2	85.5	86.0	86.5	87.2	87.7	88.2	114.5
400	91.5	91.9	90.0	89.4	89.2	88.9	88.4	87.4	87.4	117.2
500	94.9	94.5	92.4	91.9	91.9	91.2	90.0	89.9	90.2	119.7
630	96.4	96.2	93.0	92.4	92.7	92.5	92.2	92.5	92.9	121.0
800	101.9	100.7	97.0	95.9	96.0	96.2	95.9	96.4	96.5	125.1
1 000	106.0	102.7	100.7	98.9	98.5	98.4	98.7	100.0	100.5	128.2
1 250	107.1	105.2	102.2	100.1	99.9	99.7	100.1	100.1	100.2	129.6
1 600	108.7	106.2	105.6	103.4	102.1	101.2	100.6	100.7	100.9	131.6
2 000	110.4	109.3	106.9	105.3	104.6	102.1	101.9	101.3	102.6	133.5
2 500	112.8	111.9	109.4	107.1	105.4	104.3	103.1	102.3	104.9	135.7
3 150	115.3	114.8	111.6	109.5	107.0	105.0	104.3	105.8	106.1	138.0
4 000	116.0	115.2	112.2	110.0	107.8	105.0	106.3	106.2	105.7	138.6
5 000	115.7	116.4	112.7	109.9	107.7	105.7	105.6	107.6	106.7	139.0
6 300	116.6	117.5	113.8	110.0	107.8	106.6	106.3	107.8	107.5	139.8
8 000	117.0	117.4	113.9	110.4	109.2	106.5	108.2	108.2	107.9	140.1
10 000	116.8	117.6	114.1	110.5	109.5	107.1	109.1	108.0	108.5	140.3
12 500	116.4	117.1	113.9	111.1	110.6	108.2	110.1	107.9	109.2	140.3
16 000	115.4	116.2	113.4	110.9	109.9	107.7	109.1	106.6	108.4	139.6
20 000	114.2	115.2	112.9	110.7	108.9	107.6	107.4	105.4	107.2	138.8
Overall	126.1	126.4	123.2	120.4	119.0	117.1	117.8	117.3	117.9	149.5

TABLE II. - Continued. DETAILED ACOUSTIC DATA

Run 9										
Spacing ratio, X/D_h, -0.168					Reverser and nozzle vertical					
Pressure ratio, P_n/P_a, 2.55					Nozzle jet velocity, U_j, 363 m/sec					
Nozzle inlet temperature, T_n, 279 K					Ambient temperature, T_a, 278 K					
Ambient pressure, P_a, 98.2 kN/m^2 abs					Relative humidity, 52 percent					
1/3-Octave-band center frequency, f_c, Hz	Angle from nozzle axis, θ, deg									Power level, PWL, dB re 10^{-13} W
	20	40	60	80	100	120	140	160	180	
	Sound pressure level on 3.05-m radius, SPL, dB re 20μN/m^2									
50	101.8	76.0	78.8	72.2	72.0	71.7	71.8	72.0	73.5	-----
63	99.5	78.2	78.2	76.3	75.5	75.7	76.2	75.3	74.3	-----
80	95.2	79.0	80.2	77.7	78.0	77.3	76.3	78.2	77.3	-----
100	94.5	79.3	80.5	79.2	79.0	78.5	78.3	77.8	77.8	-----
125	92.0	82.7	82.5	81.2	80.0	78.5	79.7	79.0	80.7	-----
160	90.3	86.2	84.7	82.2	81.0	79.8	79.5	78.8	78.8	-----
200	89.8	89.3	88.7	87.2	86.5	85.2	84.8	84.2	83.8	-----
250	90.7	91.2	90.8	90.7	90.5	90.2	89.8	89.2	89.3	118.0
315	88.3	90.0	90.3	90.5	90.5	90.5	90.3	90.5	90.7	117.8
400	90.0	91.4	90.0	88.0	87.5	87.4	87.0	87.9	88.2	116.3
500	91.2	94.0	94.4	94.2	94.2	93.2	93.0	91.9	91.9	121.1
630	91.4	94.0	93.9	93.9	93.7	93.2	93.5	93.9	94.2	121.1
800	93.2	96.9	96.9	96.7	97.0	96.5	96.5	96.5	96.4	124.1
1 000	95.7	99.9	99.4	98.5	98.0	97.2	97.7	98.7	99.0	125.9
1 250	98.4	102.2	102.2	101.1	99.7	99.6	99.4	99.4	99.7	128.1
1 600	99.1	104.6	105.4	103.2	101.7	100.6	100.4	100.1	99.6	130.2
2 000	103.1	107.6	108.4	106.6	104.8	103.6	102.1	101.8	101.6	133.2
2 500	105.3	108.9	111.3	108.6	106.3	105.1	103.8	102.3	102.3	135.2
3 150	109.1	110.5	115.0	111.8	109.3	107.5	106.3	104.1	103.5	138.3
4 000	111.3	112.0	116.3	113.2	110.7	108.3	106.7	105.7	104.7	139.7
5 000	112.6	111.9	116.9	113.6	111.4	108.9	107.1	105.9	105.4	140.2
6 300	114.6	112.3	117.8	114.8	112.1	110.8	107.8	106.3	106.1	141.2
8 000	117.2	112.4	117.9	115.4	113.4	111.5	108.5	106.7	106.5	141.9
10 000	115.0	111.6	117.3	114.6	112.6	110.8	109.0	106.8	107.1	141.1
12 500	114.6	111.1	116.7	114.7	112.9	111.4	109.7	106.7	108.1	141.0
16 000	113.1	109.7	115.1	113.4	111.9	111.1	109.9	106.6	108.9	139.8
20 000	111.6	109.7	114.1	112.9	111.2	110.9	109.9	106.7	108.9	139.2
Overall	123.5	121.6	126.3	123.8	121.8	120.3	118.6	116.5	117.1	150.3

TABLE II. - Continued. DETAILED ACOUSTIC DATA

Run 10 - No shield	
Spacing ratio, X/D_h, -0.168	Normal horizontal position
Pressure ratio, P_n/P_a, 2.54	Nozzle jet velocity, U_j, 358 m/sec
Nozzle inlet temperature, T_n, 273 K	Ambient temperature, T_a, 267 K
Ambient pressure, P_a, 100.8 kN/m^2 abs	Relative humidity, 73 percent

1/3-Octave-band center frequency, f_c, Hz	Angle from nozzle axis, θ, deg; Sound pressure level on 3.05-m radius, SPL, dB re 20 $\mu N/m^2$											Power level, PWL, dB re 10^{-13} W for $\theta = 20^\circ$ to 160°
	20	40	60	80	100	120	140	160	180	260	280	
50	90.0	84.2	76.8	75.7	73.5	72.3	70.3	71.0	71.2	74.8	76.8	-----
63	88.7	84.0	78.3	77.8	76.7	76.2	75.7	75.2	73.7	75.5	76.8	-----
80	87.0	84.5	78.8	78.7	77.3	75.7	73.7	74.2	74.2	78.7	80.5	-----
100	85.0	84.7	81.0	80.3	79.2	78.2	76.3	76.2	75.7	79.7	81.0	108.2
125	83.0	85.5	81.2	80.8	79.5	78.0	77.0	77.0	75.7	80.0	80.3	108.3
160	84.3	86.3	82.3	82.3	81.2	80.2	79.0	79.5	78.7	81.2	81.5	109.7
200	88.2	88.5	84.8	84.2	83.3	83.0	82.5	82.5	82.0	82.8	83.7	112.2
250	90.7	90.8	88.0	86.7	86.3	86.2	85.5	86.2	85.5	86.3	87.2	115.0
315	90.4	91.2	88.7	87.9	87.7	87.5	87.4	87.9	87.5	88.7	88.9	115.9
400	89.2	91.9	89.0	87.7	87.2	86.5	86.4	87.2	87.2	88.0	88.9	115.7
500	93.7	94.2	92.0	92.0	92.4	91.5	90.5	90.5	90.7	92.0	91.7	119.5
630	94.5	96.0	93.4	93.2	93.2	93.5	92.9	93.5	93.5	93.0	93.2	121.1
800	99.5	100.0	96.9	98.5	98.7	97.5	96.9	96.5	97.0	98.7	97.5	125.5
1 000	102.9	102.1	100.9	100.2	100.4	100.9	100.1	99.9	99.6	99.6	99.6	128.2
1 250	104.1	105.7	102.9	101.9	101.7	102.4	102.1	100.9	100.6	101.1	101.2	130.1
1 600	105.6	107.6	103.9	103.8	102.9	103.1	102.8	101.9	100.6	101.6	102.4	131.5
2 000	107.0	109.8	107.3	106.5	105.8	104.1	104.5	102.3	104.6	102.6	105.1	133.7
2 500	107.5	111.5	109.8	108.3	107.5	105.1	104.8	103.6	106.3	103.8	106.1	135.4
3 150	109.9	113.9	113.5	110.5	109.7	107.2	105.7	105.5	107.2	105.9	109.2	138.0
4 000	110.7	115.1	113.7	111.2	110.2	108.2	105.2	106.1	107.1	106.9	110.4	138.6
5 000	112.5	117.0	113.3	112.3	110.5	108.1	106.5	108.0	107.3	107.6	110.8	139.5
6 300	113.2	118.0	113.4	111.9	109.7	109.4	107.2	109.2	108.2	108.4	111.9	139.9
8 000	113.3	118.3	114.1	112.5	110.8	110.5	107.5	110.0	109.0	109.3	113.0	140.5
10 000	112.8	118.8	113.8	112.6	110.6	110.3	108.4	111.4	109.9	110.6	113.1	140.6
12 500	113.1	118.9	113.7	112.6	110.7	110.9	110.4	112.1	110.9	112.2	112.9	140.9
16 000	112.1	116.9	113.3	111.9	110.4	110.8	110.8	112.4	111.6	111.1	112.6	140.0
20 000	110.7	116.3	112.5	111.2	109.0	110.5	110.3	111.3	110.5	110.2	111.5	139.2
Overall	122.3	127.2	123.5	122.0	120.4	119.8	118.7	120.1	119.5	119.6	121.8	149.8

TABLE II. - Continued. DETAILED ACOUSTIC DATA

Run 11 - Shield to center plane of nozzle and reverser											
Spacing ratio, X/D_h, -0.168						Normal horizontal position					
Pressure ratio, P_n/P_a, 2.54						Nozzle jet velocity, U_j, 357 m/sec					
Nozzle inlet temperature, T_n, 273 K						Ambient temperature, T_a, 267 K					
Ambient pressure, P_a, 100.8 kN/m^2 abs						Relative humidity, 73 percent					
1/3-Octave-band center frequency, f_c, Hz	Angle from nozzle axis, θ, deg										
	20	40	60	80	100	120	140	160	180	260	280
	Sound pressure level on 3.05-m radius, SPL, dB re $20 \mu N/m^2$										
50	89.7	82.7	77.2	75.7	74.3	72.2	70.5	70.2	72.5	75.5	77.0
63	86.7	85.2	78.7	78.2	77.5	75.8	76.0	75.0	73.5	76.0	76.7
80	85.2	83.8	78.8	78.5	77.3	76.5	74.2	74.0	74.5	79.0	80.0
100	83.7	84.5	80.5	81.2	80.3	78.8	76.8	75.7	75.7	80.0	80.7
125	83.5	85.7	81.0	80.5	80.0	78.7	77.0	76.3	76.3	80.0	80.3
160	84.8	86.5	82.5	81.3	81.2	80.0	79.7	79.0	78.5	81.3	81.7
200	88.7	88.7	84.3	82.8	82.2	82.2	82.5	82.0	81.7	83.2	83.8
250	91.0	90.3	87.7	86.0	85.3	85.2	85.2	85.2	85.3	87.0	87.7
315	90.5	90.5	88.0	87.0	86.5	86.5	86.2	87.0	87.7	89.9	90.4
400	89.7	90.9	88.5	87.4	86.2	85.4	85.4	86.2	87.5	89.4	90.0
500	94.0	93.5	90.7	89.0	89.2	88.9	88.9	89.7	91.0	92.7	92.0
630	94.5	95.5	91.5	90.2	90.2	89.4	90.9	92.7	93.9	95.5	94.9
800	99.7	99.0	94.9	93.7	92.5	92.2	94.4	95.5	97.0	99.7	99.2
1 000	103.6	101.6	98.2	96.9	96.2	95.2	97.7	98.7	100.1	102.4	101.4
1 250	104.6	104.6	101.4	99.7	98.7	96.7	99.4	100.2	100.6	102.6	102.7
1 600	106.9	106.1	102.6	101.3	98.8	98.1	99.4	100.6	100.4	103.9	104.8
2 000	108.6	109.0	105.1	103.3	100.5	99.6	101.0	101.3	104.1	104.6	107.3
2 500	109.8	110.8	106.5	103.6	102.1	100.6	100.5	103.5	106.6	105.8	108.5
3 150	112.4	113.0	109.7	105.5	103.7	101.9	102.2	104.7	106.9	108.5	111.2
4 000	112.7	114.4	109.9	106.1	105.4	102.7	102.7	105.9	107.4	109.4	112.2
5 000	113.1	116.5	110.5	106.3	104.8	103.8	103.6	108.1	107.6	109.6	112.8
6 300	114.0	117.7	110.7	107.0	105.0	104.9	104.9	108.9	108.2	110.2	113.9
8 000	114.3	118.5	111.5	108.5	107.5	105.6	105.6	110.0	109.3	111.1	114.6
10 000	113.8	119.3	112.1	109.4	107.6	106.8	105.9	111.1	109.9	112.1	115.1
12 500	113.7	118.6	112.4	110.4	107.7	107.2	108.1	111.7	111.2	113.1	114.9
16 000	112.9	117.3	112.1	109.9	107.3	106.9	107.8	111.9	111.4	112.6	113.8
20 000	112.2	116.5	111.5	109.3	106.2	106.7	107.7	111.3	110.8	111.7	112.7
Overall	123.4	127.0	121.2	118.4	116.4	115.6	116.0	119.8	119.6	121.2	123.6

TABLE II. - Continued. DETAILED ACOUSTIC DATA

Run 12 - Shield to 0.64 cm above reverser lip											
Spacing ratio, X/D_h, -0.168						Normal horizontal position					
Pressure ratio, P_n/P_a, 2.54						Nozzle jet velocity, U_j, 356 m/sec					
Nozzle inlet temperature, T_n, 274 K						Ambient temperature, T_a, 267 K					
Ambient pressure, P_a, 100.8 kN/m^2 abs						Relative humidity, 73 percent					
1/3-Octave-band center frequency, f_c, Hz	Angle from nozzle axis, θ, deg										
	20	40	60	80	100	120	140	160	180	260	280
	Sound pressure level on 3.05-m radius, SPL, dB re 20 $\mu N/m^2$										
50	88.0	83.7	76.0	75.3	74.2	73.2	70.7	70.0	70.2	75.3	77.0
63	86.5	82.7	78.7	78.2	77.3	76.8	75.8	75.3	72.8	75.8	77.5
80	83.3	82.7	79.2	78.3	77.7	77.2	74.5	74.3	73.2	79.3	80.3
100	82.8	83.8	81.0	81.2	80.7	79.0	77.2	75.7	75.3	79.7	80.7
125	83.2	83.8	81.0	80.8	79.8	78.7	77.2	76.3	75.8	79.8	80.3
160	85.0	85.7	82.8	82.0	81.7	80.3	79.3	79.3	78.3	81.3	81.5
200	88.5	87.5	84.5	83.3	82.8	82.2	82.3	82.0	81.7	83.0	83.3
250	90.7	89.5	87.3	86.2	85.2	84.8	84.3	85.0	85.5	87.3	87.7
315	90.7	90.2	87.9	86.9	86.2	85.7	85.9	86.9	88.0	90.0	90.7
400	89.4	90.4	88.4	87.0	85.9	85.2	85.7	86.4	87.5	89.9	90.0
500	94.0	93.4	90.4	88.5	88.4	87.9	88.9	89.9	91.2	93.2	93.0
630	95.2	95.0	92.2	90.2	90.0	89.4	90.7	92.7	93.9	95.5	95.2
800	100.0	98.7	95.0	93.5	92.5	91.7	93.9	95.5	97.2	100.2	99.2
1 000	103.2	100.7	98.6	96.1	95.4	94.9	97.6	98.7	100.1	102.6	101.6
1 250	104.9	104.1	101.1	98.4	97.4	96.7	99.2	99.7	100.7	102.6	103.2
1 600	107.4	106.4	101.6	99.6	98.8	96.9	98.1	100.4	100.6	104.3	104.1
2 000	108.6	109.0	104.6	102.1	99.6	98.6	99.8	101.3	104.0	105.5	107.3
2 500	109.0	111.0	106.0	102.6	101.0	100.5	100.0	103.0	106.5	106.1	108.5
3 150	111.0	113.2	109.5	104.7	102.9	101.7	102.2	104.7	106.9	108.7	111.2
4 000	112.4	114.4	109.7	104.4	105.1	102.2	102.4	105.6	107.4	109.6	112.1
5 000	114.0	116.1	109.8	104.3	103.0	102.5	104.0	107.6	107.6	110.1	112.8
6 300	114.2	117.0	109.7	105.0	103.0	103.4	103.9	108.5	108.0	110.5	113.9
8 000	114.0	117.8	110.8	106.0	105.0	104.3	105.0	109.6	109.5	111.6	114.6
10 000	113.6	118.1	110.8	106.3	104.6	105.4	105.8	110.6	110.1	112.6	114.9
12 500	114.1	118.2	110.9	106.7	104.1	106.7	106.9	111.2	111.4	113.4	115.1
16 000	112.8	116.9	110.6	106.3	103.1	106.4	107.1	111.6	111.3	112.4	113.9
20 000	111.8	115.7	109.7	105.7	101.5	106.2	107.5	110.8	110.7	111.8	112.8
Overall	123.4	126.5	120.2	115.9	114.1	114.8	115.5	119.4	119.6	121.5	123.6

TABLE II. - Continued. DETAILED ACOUSTIC DATA

Run 13 - Shield to 8.26 cm above reverser lip											
Spacing ratio, X/D_h, -0.168						Normal horizontal position					
Pressure ratio, P_n/P_a, 2.54						Nozzle jet velocity, U_j, 356 m/sec					
Nozzle inlet temperature, T_n, 274 K						Ambient temperature, T_a, 267 K					
Ambient pressure, P_a, 100.8 kN/m^2 abs						Relative humidity, 73 percent					
1/3-Octave-band center frequency, f_c, Hz	Angle from nozzle axis, θ, deg										
	20	40	60	80	100	120	140	160	180	260	280
	Sound pressure level on 3.05-m radius, SPL, dB re 20 μN/m^2										
50	-----	82.7	77.0	75.8	74.0	74.0	71.8	71.2	71.2	74.0	76.5
63	81.2	82.5	78.7	78.3	77.3	77.8	76.7	75.0	73.5	75.0	76.8
80	83.0	83.3	79.8	79.0	78.2	77.7	75.3	74.5	74.3	79.0	80.3
100	82.7	84.5	81.2	81.3	80.7	79.2	77.7	75.8	75.3	79.5	80.5
125	83.0	84.5	81.2	80.7	79.8	78.8	77.2	76.7	75.7	79.8	80.7
160	84.5	85.8	82.5	81.8	81.3	80.5	79.3	79.3	78.3	81.2	81.7
200	87.8	88.0	84.8	83.2	82.2	82.0	81.8	81.8	82.2	82.8	83.3
250	90.8	90.3	87.3	86.0	85.5	85.2	84.7	85.0	85.8	87.3	88.2
315	90.7	90.9	87.5	86.7	86.0	85.9	85.4	87.0	87.9	90.5	90.2
400	89.7	90.9	88.4	87.4	86.2	85.5	85.7	86.4	87.4	90.2	90.0
500	94.0	93.4	90.5	88.7	87.9	87.9	88.7	89.5	91.2	93.0	93.0
630	94.7	95.2	91.7	90.0	89.7	89.5	90.5	92.5	93.9	96.0	95.4
800	100.2	99.0	94.7	93.5	92.2	91.9	93.7	95.9	97.7	100.5	99.4
1 000	103.4	100.7	98.2	96.2	94.6	94.9	97.2	98.6	100.1	103.6	102.1
1 250	104.7	103.9	101.1	97.4	96.4	96.9	98.4	99.4	100.7	102.6	103.2
1 600	107.1	106.1	101.9	98.9	97.9	96.6	97.3	100.3	100.6	104.4	104.4
2 000	109.0	108.8	104.1	101.6	99.1	98.6	99.6	101.1	104.1	105.3	107.6
2 500	110.0	110.5	106.1	102.1	101.0	99.1	100.0	102.6	106.6	106.1	108.3
3 150	112.4	113.0	109.7	104.0	102.9	101.4	102.5	104.7	107.4	108.9	110.9
4 000	113.2	114.2	109.4	103.6	104.4	102.2	102.1	105.2	107.2	109.4	112.2
5 000	113.5	116.5	109.6	103.8	103.0	102.6	103.3	107.5	107.8	110.1	112.6
6 300	114.5	117.4	109.5	105.4	103.0	103.9	104.2	108.9	108.4	110.4	113.9
8 000	114.3	118.3	110.6	105.1	104.0	104.5	105.1	109.6	109.1	111.6	114.6
10 000	114.1	118.6	110.8	105.6	103.6	105.4	105.3	110.9	110.1	112.4	114.6
12 500	114.4	118.7	110.6	105.7	102.7	106.4	106.6	111.6	111.2	113.4	114.6
16 000	113.3	117.1	110.3	105.3	101.6	105.9	106.4	111.9	111.6	112.8	113.8
20 000	112.3	115.8	109.5	104.5	99.8	105.7	107.0	110.8	110.7	111.8	112.7
Overall	123.8	126.8	120.1	115.2	113.4	114.6	115.2	119.5	119.7	121.5	123.4

TABLE II. - Continued. DETAILED ACOUSTIC DATA

Run 14 - Shield to 15.9 cm above reverser lip											
Spacing ratio, X/D_h, -0.168						Normal horizontal position					
Pressure ratio, P_n/P_a, 2.54						Nozzle jet velocity, U_j, 356 m/sec					
Nozzle inlet temperature, T_n, 274 K						Ambient temperature, T_a, 267 K					
Ambient pressure, P_a, 100.8 kN/M^2 abs						Relative humidity, 73 percent					
1/3-Octave-band center frequency, f_c, Hz	Angle from nozzle axis, θ, deg										
	20	40	60	80	100	120	140	160	180	260	280
	Sound pressure level on 3.05-m radius, SPL, dB re 20 $\mu N/m^2$										
50	89.7	83.7	77.5	75.5	74.7	73.7	70.2	69.8	70.5	75.0	76.7
63	87.7	82.7	78.8	78.2	77.5	76.5	75.0	74.5	73.2	75.5	77.0
80	86.7	83.8	79.5	79.2	77.8	77.0	74.8	73.5	74.0	79.5	79.7
100	84.0	84.2	80.8	81.5	80.5	78.8	77.3	75.0	75.0	80.5	80.7
125	83.5	85.7	81.2	80.8	80.0	78.8	77.5	76.3	75.7	79.7	80.3
160	84.8	86.3	82.3	81.8	81.3	80.3	79.2	78.8	78.8	81.3	81.7
200	88.2	88.2	84.7	83.3	82.5	82.0	81.8	81.8	81.5	83.3	83.5
250	90.8	90.2	87.3	86.0	85.0	84.8	84.7	85.2	85.7	87.7	88.2
315	90.2	90.9	87.5	86.7	86.4	85.4	85.9	86.7	88.0	90.4	91.0
400	89.5	90.5	88.4	87.4	86.4	85.9	86.2	86.2	87.4	90.2	90.2
500	93.7	92.9	90.4	88.4	87.5	87.9	88.5	89.2	91.2	93.2	93.2
630	94.5	95.4	91.2	90.2	90.2	89.9	90.4	92.2	94.0	96.4	95.7
800	99.5	99.0	94.7	93.4	92.5	92.0	93.4	95.7	97.5	100.4	99.2
1 000	102.6	100.7	98.2	96.6	94.6	93.9	97.1	97.7	100.1	103.7	102.1
1 250	104.4	103.9	100.9	97.4	95.9	95.7	97.9	99.4	100.6	102.2	103.6
1 600	106.8	105.9	101.1	98.6	96.6	96.4	96.8	100.1	100.6	104.4	104.6
2 000	108.5	108.8	104.1	101.5	98.5	98.0	99.8	101.1	104.3	105.3	107.6
2 500	109.8	110.1	106.0	101.8	100.6	99.1	99.8	102.6	106.5	106.0	108.1
3 150	111.7	113.2	109.4	103.5	102.0	101.2	102.0	104.5	107.2	108.7	111.2
4 000	113.1	114.4	109.2	103.6	104.2	102.2	102.4	105.4	107.6	109.7	112.2
5 000	113.3	116.6	109.8	103.6	102.6	102.6	103.3	107.5	107.5	110.0	112.8
6 300	114.0	117.9	109.4	104.5	102.7	103.2	104.0	108.9	108.4	110.4	113.9
8 000	114.0	118.5	110.5	105.0	103.5	104.1	105.0	109.6	109.3	111.6	114.6
10 000	113.4	118.8	110.4	105.4	103.1	105.3	105.6	111.1	110.4	112.4	114.9
12 500	113.7	118.6	110.6	105.2	102.6	106.2	107.1	111.9	111.4	113.6	114.6
16 000	113.1	117.1	110.6	105.3	100.9	106.3	106.6	111.9	111.4	112.9	113.9
20 000	112.0	116.0	109.7	104.2	99.5	105.8	106.8	111.2	111.2	111.8	112.7
Overall	123.4	126.9	120.0	114.9	112.9	114.5	115.2	119.6	119.8	121.6	123.5

TABLE II. - Continued. DETAILED ACOUSTIC DATA

Run 15 - Shield to 15.9 cm above reverser lip and extended 15.2 cm forward											
Spacing ratio, X/D_h, -0.168						Normal horizontal position					
Pressure ratio, P_n/P_a, 2.54						Nozzle jet velocity, U_j, 356 m/sec					
Nozzle inlet temperature, T_n, 274 K						Ambient temperature, T_a, 267 K					
Ambient pressure, P_a, 100.8 kN/m^2 abs						Relative humidity, 73 percent					
1/3-Octave-band center frequency, f_c, Hz	Angle from nozzle axis, θ, deg										
	20	40	60	80	100	120	140	160	180	260	280
	Sound pressure level on 3.05-m radius, SPL, dB re 20 $\mu N/m^2$										
50	90.5	81.0	77.7	76.3	75.2	73.5	70.5	70.7	70.5	74.8	77.2
63	88.5	83.0	80.7	78.8	78.5	77.0	75.5	75.0	72.2	77.2	77.7
80	86.5	83.5	80.0	79.0	78.5	77.0	74.5	74.7	73.7	79.2	80.7
100	84.0	83.8	81.7	82.8	81.3	79.8	78.2	76.5	75.5	81.0	81.5
125	83.5	83.5	81.5	81.0	80.5	78.5	77.5	76.7	77.0	80.8	80.5
160	84.8	84.5	82.5	82.0	81.5	80.3	79.2	79.2	79.0	81.5	81.8
200	88.8	87.8	85.8	85.3	84.7	83.7	82.3	82.0	82.2	83.3	83.5
250	90.3	89.0	87.8	87.0	86.5	85.3	84.5	85.2	85.3	87.2	87.8
315	90.0	89.0	87.5	86.7	85.7	85.0	85.5	86.4	87.9	90.9	91.2
400	89.2	89.9	88.7	87.4	86.0	84.9	85.2	86.2	87.0	90.0	91.0
500	93.7	92.0	89.9	87.0	87.5	87.4	88.0	89.7	90.9	94.0	94.2
630	94.5	93.2	92.0	90.0	89.0	89.5	91.5	92.9	93.9	95.9	96.7
800	99.9	97.2	94.7	92.0	92.7	93.0	94.9	96.0	97.2	99.0	99.2
1 000	102.2	99.9	97.6	94.9	95.9	95.9	97.9	99.2	99.9	102.9	102.6
1 250	103.7	101.9	99.9	97.1	97.4	97.6	100.2	100.6	100.2	102.9	103.1
1 600	106.6	104.4	99.9	97.6	97.8	98.9	99.6	100.9	100.8	104.1	104.8
2 000	108.0	106.6	102.0	99.0	98.3	98.6	101.1	101.1	104.6	105.8	107.8
2 500	109.3	108.6	103.6	100.5	99.1	99.1	101.1	103.0	106.3	106.3	108.3
3 150	111.5	111.0	107.2	102.2	101.9	100.9	102.9	104.7	107.2	108.5	111.2
4 000	112.6	111.9	107.2	102.2	102.9	101.4	102.6	106.2	107.6	109.4	112.4
5 000	113.1	113.3	107.0	102.0	101.8	102.6	104.0	107.5	108.1	110.1	113.1
6 300	114.0	114.9	107.5	102.7	102.0	102.7	104.4	109.0	108.5	110.5	114.2
8 000	113.8	115.3	108.5	103.0	102.5	104.5	104.6	110.0	109.5	111.6	114.6
10 000	113.8	116.4	108.8	103.6	102.3	105.6	106.3	111.1	110.1	112.4	115.1
12 500	114.2	116.4	108.9	103.4	101.6	106.7	108.2	111.9	111.2	113.2	114.7
16 000	113.4	114.6	107.9	102.6	100.4	107.3	109.1	112.1	111.6	112.9	114.3
20 000	112.2	113.7	107.0	101.7	98.7	107.2	109.5	111.3	110.7	112.2	113.0
Overall	123.3	124.4	117.9	113.1	112.3	115.0	116.6	119.8	119.8	121.6	123.7

TABLE II. - Continued. DETAILED ACOUSTIC DATA

Run 16									
Slot nozzle only					Normal horizontal position				
Pressure ratio, P_n/P_a, 2.54					Nozzle jet velocity, U_j, 356 m/sec				
Nozzle inlet temperature, T_n, 274 K					Ambient temperature, T_a, 267 K				
Ambient pressure, P_a, 100.8 kN/m^2 abs					Relative humidity, 73 percent				
1/3-Octave-band center frequency, f_c, Hz	Angle from nozzle axis, θ, deg								Power level, PWL, dB re 10^{-13} W
	20	40	60	80	100	120	140	160	
	Sound pressure level on 3.05-m radius, SPL, dB re 20 μN/m^2								
50	68.2	66.3	68.5	68.0	70.3	72.7	78.0	84.0	-----
63	69.0	67.8	70.2	70.7	73.7	75.3	78.5	83.0	-----
80	71.2	69.2	70.5	71.3	74.2	75.3	78.8	84.7	-----
100	71.0	70.3	72.2	72.3	74.8	77.2	79.8	85.7	104.8
125	72.5	72.3	72.2	74.5	76.7	78.0	81.5	87.8	106.6
160	73.2	73.0	74.2	76.5	79.5	81.5	83.7	90.3	109.1
200	76.5	76.3	78.7	81.2	84.0	85.2	86.7	94.5	113.0
250	79.2	80.7	82.7	85.2	87.7	88.2	90.3	97.7	116.4
315	80.9	82.0	83.9	85.9	87.5	88.2	92.7	99.5	117.8
400	81.0	82.4	83.7	85.7	88.7	90.2	95.2	103.0	120.6
500	83.9	85.4	88.4	90.4	92.4	92.9	99.0	105.4	123.4
630	86.0	86.9	88.5	90.5	92.4	94.2	101.4	107.2	125.2
800	90.2	90.5	92.7	94.9	95.9	97.2	105.0	109.4	128.0
1 000	93.4	92.6	95.2	96.9	98.6	100.2	108.1	111.1	130.3
1 250	96.4	96.9	96.7	98.2	100.2	102.7	109.9	110.7	131.5
1 600	99.6	99.1	98.8	100.9	103.4	106.8	116.4	115.8	136.8
2 000	100.1	99.5	100.8	103.0	105.8	109.8	120.0	118.5	140.0
2 500	99.1	99.1	100.3	102.1	105.1	107.0	114.0	113.8	135.3
3 150	111.9	101.2	103.0	107.2	107.2	108.7	113.5	113.4	136.5
4 000	118.7	104.7	106.6	112.6	110.1	109.2	114.9	114.7	139.7
5 000	104.1	103.3	105.0	106.1	107.5	109.1	112.3	111.5	135.5
6 300	106.5	103.4	106.4	109.9	110.4	110.5	112.5	111.4	137.0
8 000	110.5	105.1	110.6	114.6	114.6	112.8	112.8	112.1	140.1
10 000	103.1	102.4	104.8	107.6	109.6	110.8	112.1	110.3	136.1
12 500	102.7	101.4	103.7	107.1	108.6	110.6	111.7	109.2	135.5
16 000	102.8	100.8	101.6	105.3	106.9	109.3	111.1	107.1	134.2
20 000	100.2	100.0	100.3	104.0	105.3	108.0	109.8	105.7	132.9
Overall	120.7	113.1	115.8	119.5	119.9	120.6	125.5	124.8	148.3

TABLE II. - Continued. DETAILED ACOUSTIC DATA

Run 17									
Slot nozzle only					Normal horizontal position				
Pressure ratio, P_n/P_a, 1.74					Nozzle jet velocity, U_j, 284 m/sec				
Nozzle inlet temperature, T_n, 274 K					Ambient temperature, T_a, 267 K				
Ambient pressure, P_a, 100.8 kN/m^2 abs					Relative humidity, 73 percent				
1/3-Octave-band center frequency, f_c, Hz	Angle from nozzle axis, θ, deg								Power level, PWL, dB re 10^{-13} W
	20	40	60	80	100	120	140	160	
	Sound pressure level on 3.05-m radius, SPL, dB re 20 $\mu N/m^2$								
50	60.7	60.5	59.7	59.7	61.7	65.0	67.8	73.7	-----
63	62.2	61.7	63.0	64.2	65.5	66.5	69.3	73.2	-----
80	64.5	64.2	63.5	65.0	66.2	67.0	70.2	74.7	-----
100	64.2	64.0	64.5	65.7	67.3	69.2	71.7	77.3	96.8
125	68.5	69.5	68.7	70.8	71.2	72.3	73.7	78.5	99.6
160	66.8	67.3	67.7	68.0	70.2	71.8	76.0	81.2	100.3
200	70.2	70.2	71.0	72.3	74.3	75.7	78.8	84.5	103.8
250	73.2	73.8	74.8	76.8	78.8	79.7	83.3	88.0	107.7
315	74.2	74.7	75.7	77.7	79.4	81.7	86.0	90.4	109.7
400	74.2	75.5	76.5	77.7	80.0	82.0	87.9	92.9	111.5
500	76.0	77.9	80.2	81.9	83.7	85.4	90.7	95.5	114.4
630	77.5	78.7	80.0	81.5	83.5	86.2	92.2	96.7	115.4
800	80.2	82.0	83.5	85.2	86.7	89.0	95.5	98.9	118.2
1 000	82.1	82.7	85.1	86.4	88.2	90.4	96.7	99.7	119.3
1 250	83.6	84.6	86.1	86.9	88.9	91.4	97.4	99.2	119.6
1 600	84.4	86.4	86.3	87.6	90.3	92.6	97.9	98.8	120.0
2 000	87.1	87.0	87.3	89.5	91.8	94.0	98.3	98.0	120.6
2 500	87.6	87.1	88.3	89.8	92.5	94.3	97.5	97.1	120.4
3 150	89.9	88.9	89.9	90.9	93.7	95.7	97.4	97.4	121.1
4 000	87.7	88.7	90.2	90.7	93.6	95.2	95.7	95.4	120.4
5 000	88.0	88.3	90.5	92.1	93.8	95.3	95.5	95.3	120.5
6 300	87.9	88.5	90.7	92.7	93.7	95.4	94.5	96.5	120.6
8 000	89.1	89.5	91.3	93.0	94.3	95.8	94.0	96.5	120.9
10 000	89.9	90.1	90.8	92.6	93.1	95.1	93.9	96.3	120.4
12 500	89.4	89.9	90.1	92.1	92.4	94.4	94.4	95.2	119.9
16 000	88.6	89.1	89.3	91.4	90.9	93.3	93.6	92.4	118.8
20 000	87.2	88.5	87.8	90.7	89.7	92.0	91.8	90.5	117.5
Overall	99.4	99.8	100.9	102.6	104.0	105.9	108.0	109.5	132.0

TABLE II. - Continued. DETAILED ACOUSTIC DATA

Run 18	
Slot nozzle only	Vertical position
Pressure ratio, P_n/P_a, 1.25	Nozzle jet velocity, U_j, 179 m/sec
Nozzle inlet temperature, T_n, 274 K	Ambient temperature, $T_a \cong T_n$
Ambient pressure, P_a, 100.8 kN/m^2 abs	Relative humidity, 73 percent

1/3-Octave-band center frequency, f_c, Hz	Angle from nozzle axis, θ, deg								Power level, PWL, dB re 10^{-13} W
	20	40	60	80	100	120	140	160	
	Sound pressure level on 3.05-m radius, SPL, dB re 20 $\mu N/m^2$								
50	57.0	56.7	56.0	55.8	56.2	57.3	58.5	61.5	-----
63	58.2	57.5	58.8	59.7	59.3	60.0	60.5	62.2	-----
80	62.3	61.2	61.5	62.8	62.2	61.5	62.7	64.0	-----
100	60.0	58.8	59.7	61.5	61.8	63.0	62.5	66.5	89.3
125	66.0	64.5	65.7	69.0	69.7	69.2	65.0	67.0	95.1
160	58.7	59.0	59.0	59.5	61.3	62.8	64.7	69.0	89.8
200	60.5	60.0	61.0	62.3	63.5	64.5	66.5	71.5	92.0
250	64.7	64.5	65.0	67.2	68.0	68.3	70.3	74.8	95.9
315	64.7	64.4	65.0	66.5	67.9	69.4	72.4	76.2	96.7
400	63.5	63.9	65.0	66.2	67.5	69.7	73.7	77.9	97.6
500	64.9	66.0	67.4	69.2	71.0	72.2	76.2	79.9	100.0
630	65.7	66.5	67.7	69.2	70.5	72.9	77.0	80.2	100.4
800	68.2	69.4	70.4	72.0	73.5	75.2	79.2	82.5	102.9
1 000	69.4	69.6	71.7	73.4	74.6	76.6	80.1	83.1	103.7
1 250	70.6	70.9	72.2	73.4	75.1	77.2	80.2	82.1	103.8
1 600	70.9	72.3	72.1	73.6	75.9	77.9	80.8	81.6	104.1
2 000	72.1	72.1	73.0	74.6	77.3	79.0	81.3	80.6	104.7
2 500	71.6	71.6	73.1	74.8	77.6	79.1	80.6	79.5	104.5
3 150	73.4	73.0	74.7	75.7	78.4	79.9	80.5	78.9	105.1
4 000	72.4	72.4	74.6	75.7	77.9	78.7	78.9	77.7	104.1
5 000	72.8	72.8	74.8	76.6	78.1	78.5	78.3	77.5	104.2
6 300	71.9	72.5	74.4	76.4	77.7	78.4	76.9	78.4	103.8
8 000	72.1	72.5	75.3	76.5	78.1	78.5	76.6	78.0	104.0
10 000	71.9	72.3	74.3	75.9	76.6	76.9	75.9	77.8	103.0
12 500	71.9	71.6	72.7	75.4	75.7	76.1	76.4	76.6	102.3
16 000	70.4	70.3	71.4	74.3	73.9	74.8	75.8	74.3	100.9
20 000	69.2	69.5	69.7	72.5	72.8	73.3	73.0	72.3	99.4
Overall	83.7	83.8	85.4	87.1	88.7	89.8	91.2	92.4	115.8

TABLE II. - Concluded. DETAILED ACOUSTIC DATA

Run 19 (ref. 3)	
Slot nozzle only	Vertical position
Pressure ratio, P_n/P_a, ~1.7	Nozzle jet velocity, U_j, ~ 280 m/sec
Nozzle inlet temperature, T_n, 279 K	Ambient temperature, T_a, $\cong T_n$
Ambient pressure, P_a, 101.3 kN/m^2 abs	Relative humidity, 35 percent

1/3-Octave-band center frequency, f_c, Hz	Angle from nozzle axis, θ, deg								Power level, PWL, dB re 10^{-13} W
	20	40	60	80	100	120	140	160	
	Sound pressure level on 3.05-m radius, SPL, dB re 20 $\mu N/m^2$								
50	61.5	61.0	59.7	60.5	63.7	63.8	65.7	72.0	-----
63	63.2	63.2	63.7	63.0	66.3	67.2	67.2	72.3	-----
80	70.5	70.0	71.3	70.0	70.7	71.2	71.3	75.0	-----
100	66.7	66.8	66.3	68.2	69.0	69.7	70.5	76.2	-----
125	77.0	77.5	76.3	79.0	77.5	75.7	77.3	79.5	-----
160	67.0	67.2	67.3	69.5	71.7	72.7	73.5	79.5	-----
200	69.3	69.7	71.0	74.0	76.2	76.7	76.2	83.8	-----
250	73.3	73.3	75.5	78.7	80.3	80.3	79.7	87.0	107.6
315	73.7	74.9	76.2	78.9	80.5	80.0	82.0	89.0	109.1
400	73.4	75.0	75.5	78.0	80.2	81.7	83.9	91.9	111.2
500	75.9	77.9	79.4	82.2	85.0	84.5	87.4	94.7	114.3
630	77.2	78.9	79.7	81.7	83.9	84.9	88.4	95.9	115.2
800	79.5	81.5	82.7	84.7	86.9	87.0	92.0	98.2	117.8
1 000	81.2	82.6	83.7	85.7	87.4	88.7	94.1	99.9	119.4
1 250	82.7	83.9	84.6	86.4	87.7	89.4	95.4	99.6	119.6
1 600	83.4	85.1	85.3	87.6	88.9	90.4	96.9	99.1	119.9
2 000	85.3	85.9	86.8	88.9	89.9	91.6	97.8	98.6	120.3
2 500	86.1	86.1	87.3	89.1	90.3	92.5	98.1	97.6	120.2
3 150	88.5	87.5	89.0	89.8	91.3	94.2	98.8	97.2	120.8
4 000	89.2	86.9	88.1	89.1	91.1	94.4	98.1	95.4	120.0
5 000	89.5	88.0	87.5	89.6	91.5	94.8	98.5	94.3	120.1
6 300	89.7	88.7	87.4	89.9	91.5	95.9	98.2	94.0	120.2
8 000	89.1	89.0	88.6	89.8	91.8	96.8	97.6	93.6	120.3
10 000	88.4	88.7	88.7	90.1	91.4	96.6	97.7	92.2	120.0
12 500	87.9	88.6	88.2	89.9	91.7	96.7	97.1	90.9	119.7
16 000	87.1	88.3	87.6	89.3	91.4	96.1	96.3	88.3	118.9
20 000	86.0	87.5	86.5	88.8	90.8	94.8	94.2	86.5	117.6
Overall	99.0	98.9	99.1	100.8	102.5	106.1	108.9	108.8	131.8

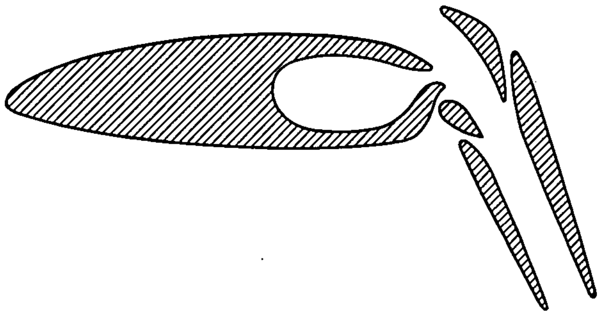

(a) Typical landing configuration.

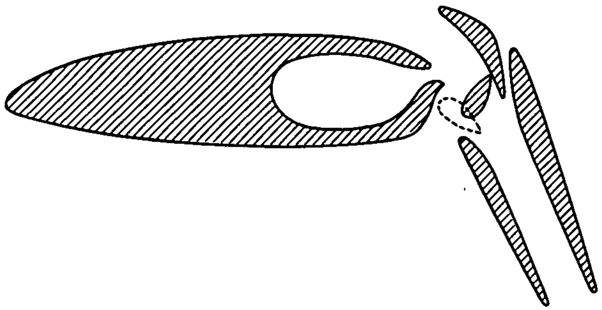

(b) Possible slot reverser configuration, V-gutter type.

Figure 1. - Augmentor-wing slot flow-reversal scheme.

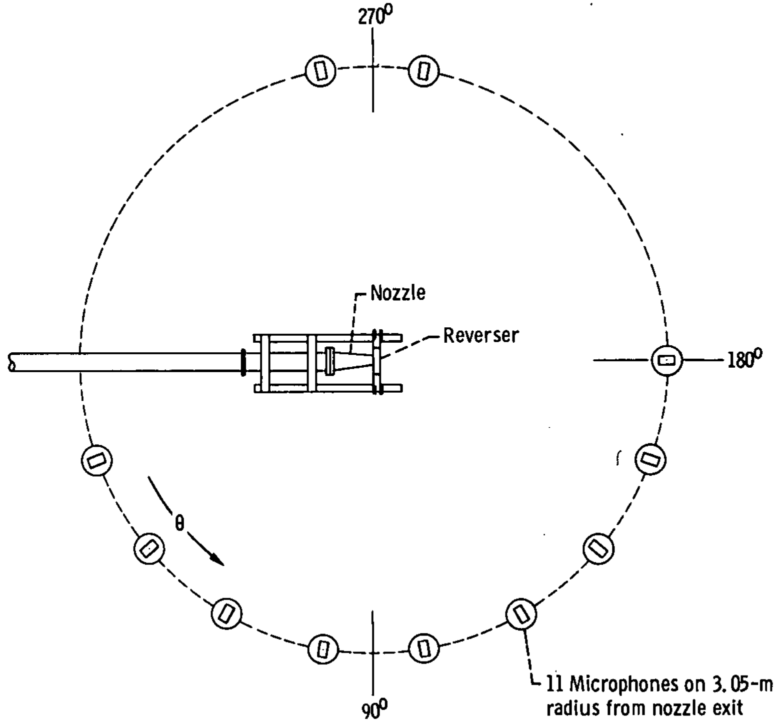

(a) Plan view.

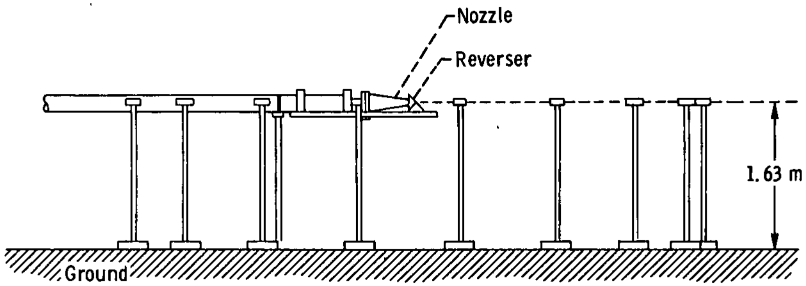

(b) Elevation.

Figure 2. - Schematic diagram of acoustic rig.

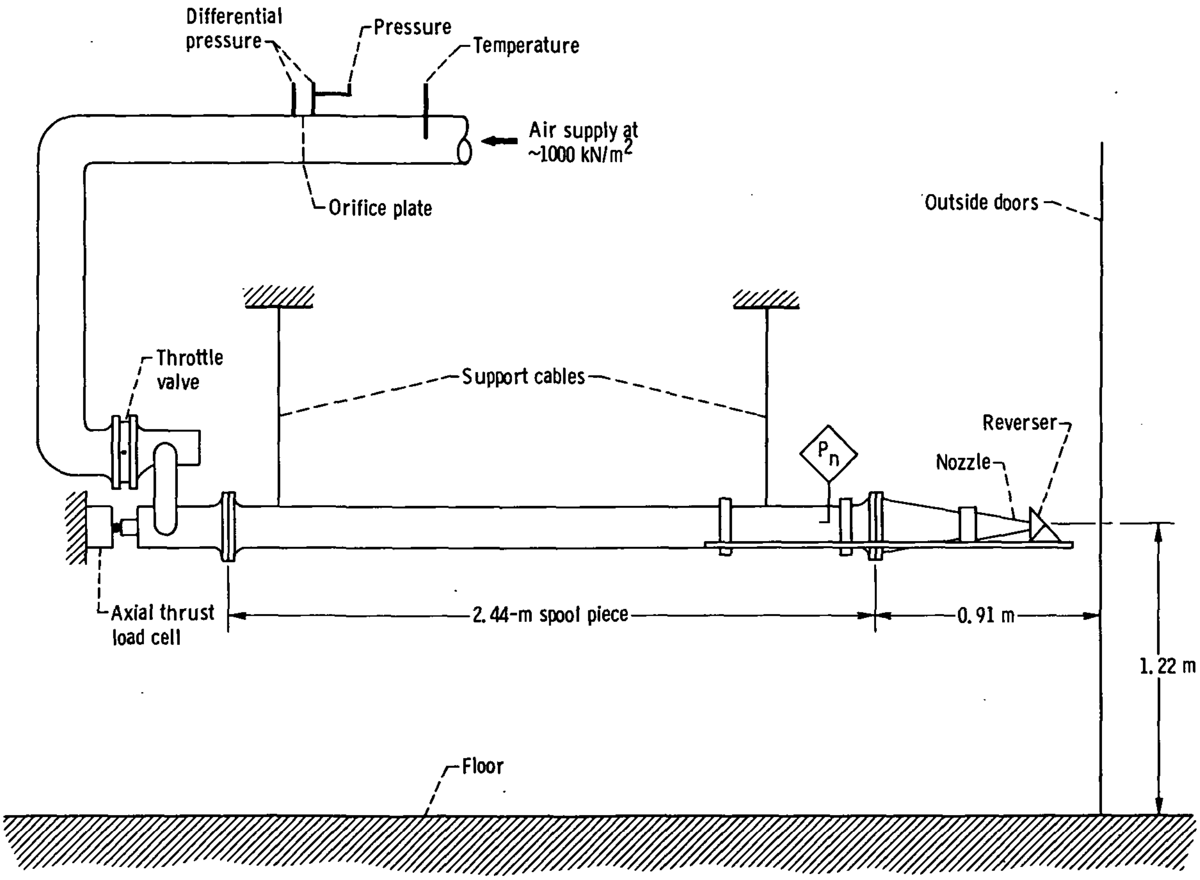

Figure 3. - Schematic diagram of airflow rig.

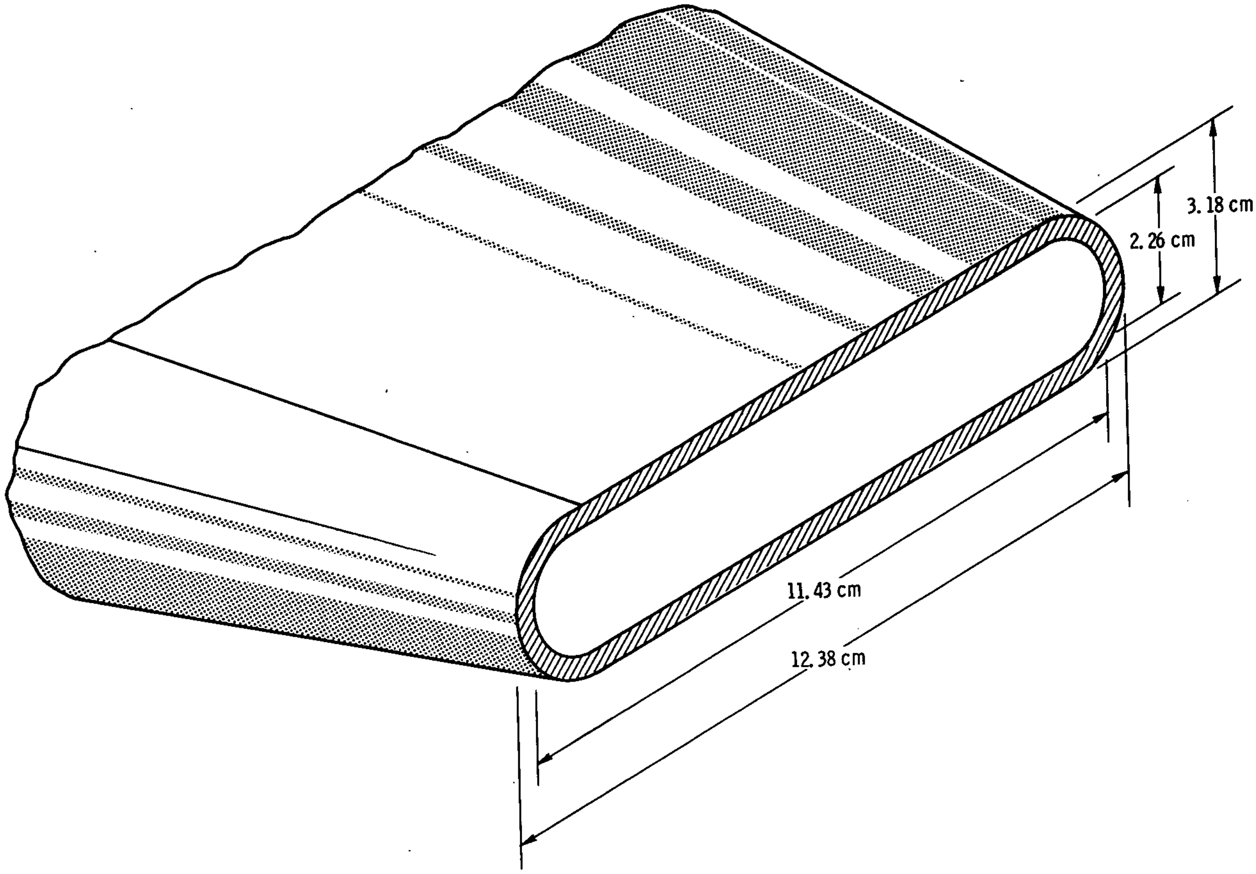

Figure 4. - Slot nozzle.

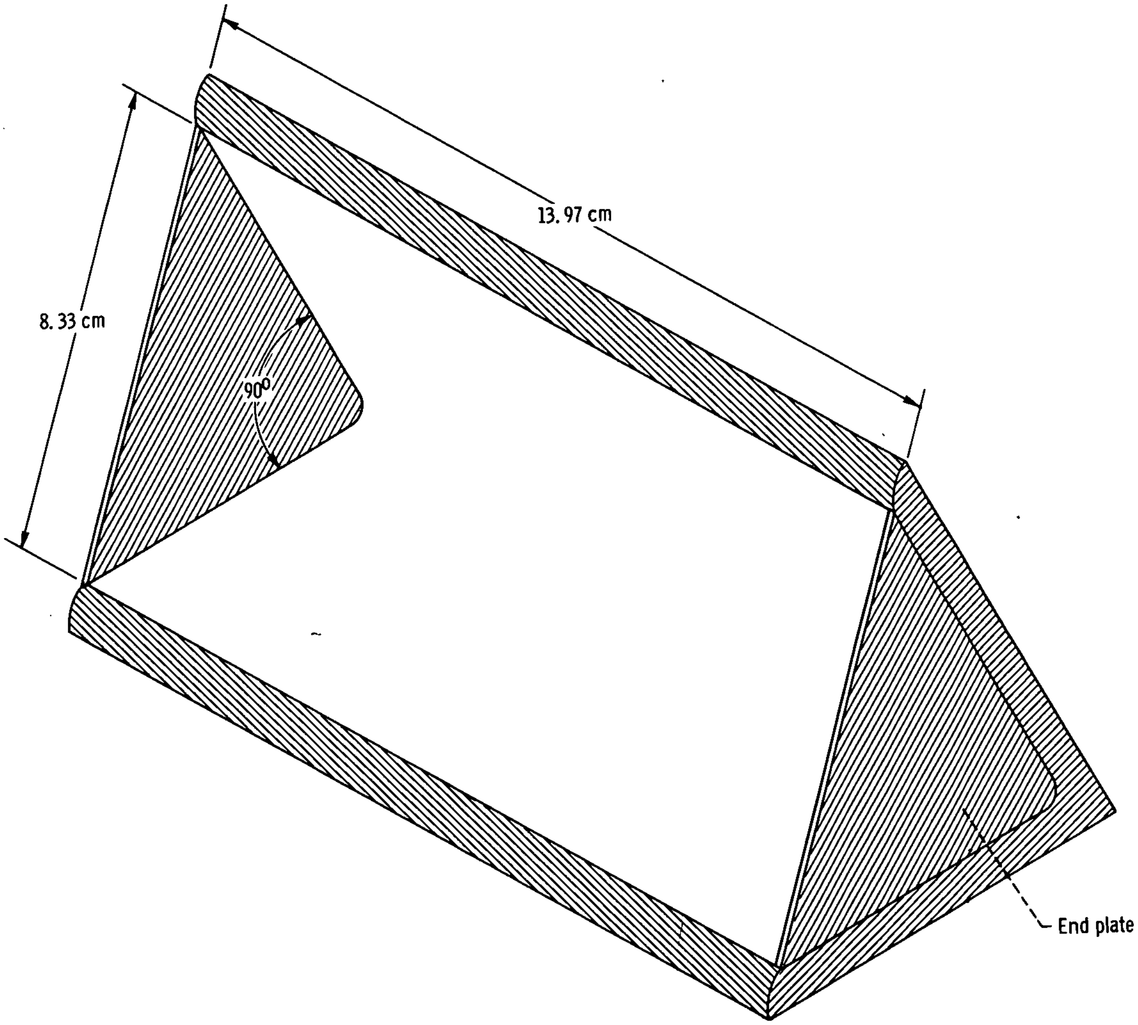

Figure 5. - V-gutter thrust reverser.

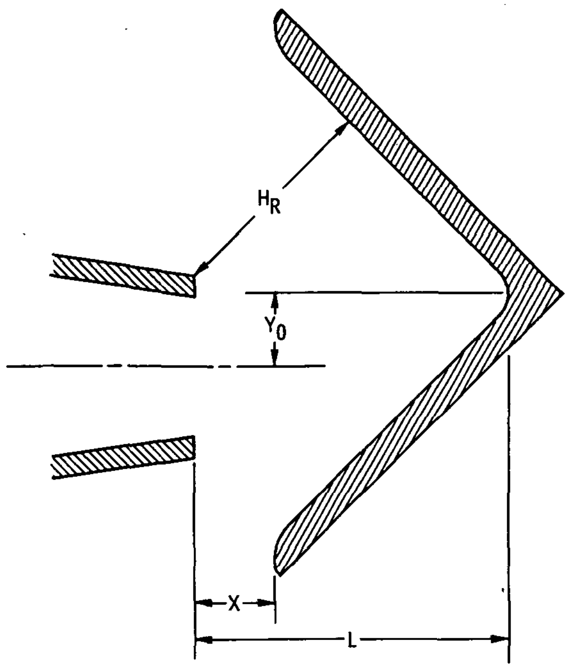

Figure 6. - Arrangement of nozzle and reverser with geometric variables.

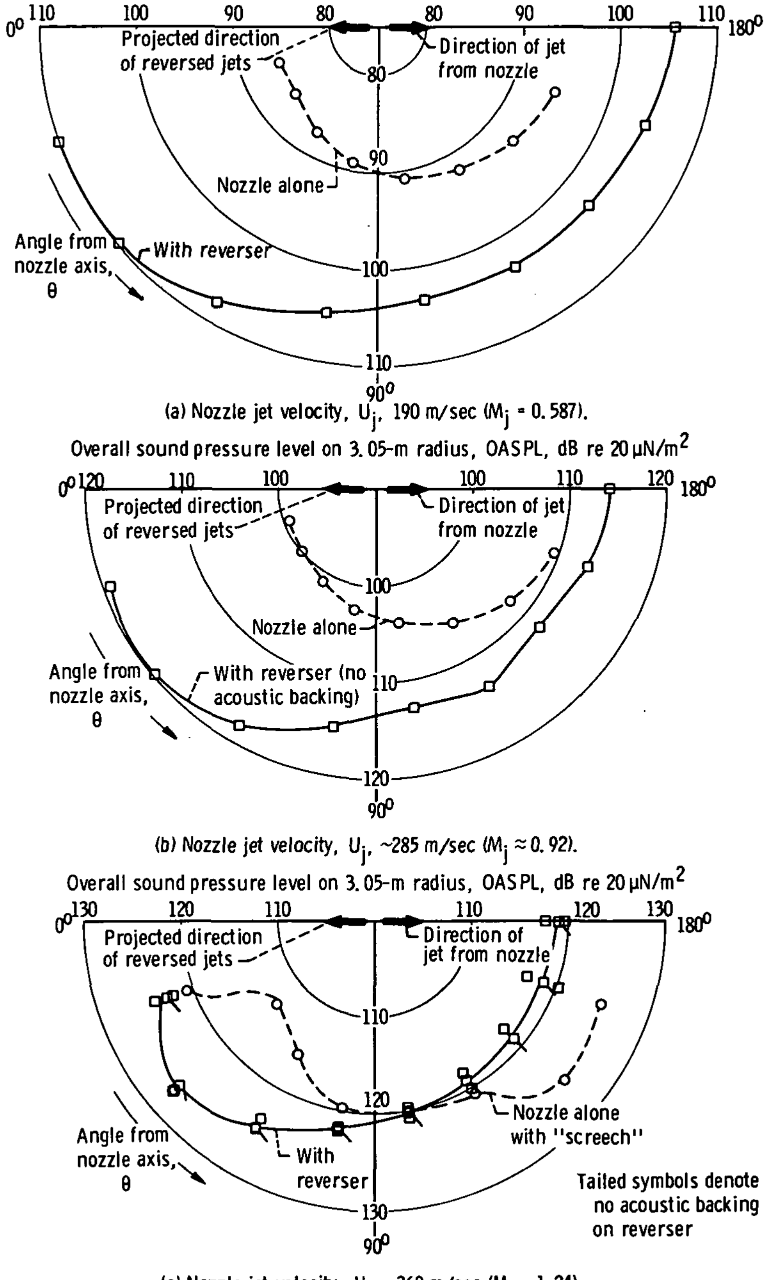

(a) Nozzle jet velocity, U_j, 190 m/sec (M_j = 0.587).

(b) Nozzle jet velocity, U_j, ~285 m/sec ($M_j \approx 0.92$).

(c) Nozzle jet velocity, U_j, ~360 m/sec (M_j ~ 1.24).

Figure 7. - Effect of thrust reversal on directivity of overall sound pressure level for 2.26- by 11.43-centimeter slot nozzle and V-gutter reverser at various velocities. Normal horizontal position; no offset; spacing ratio, X/D_h, -0.168.

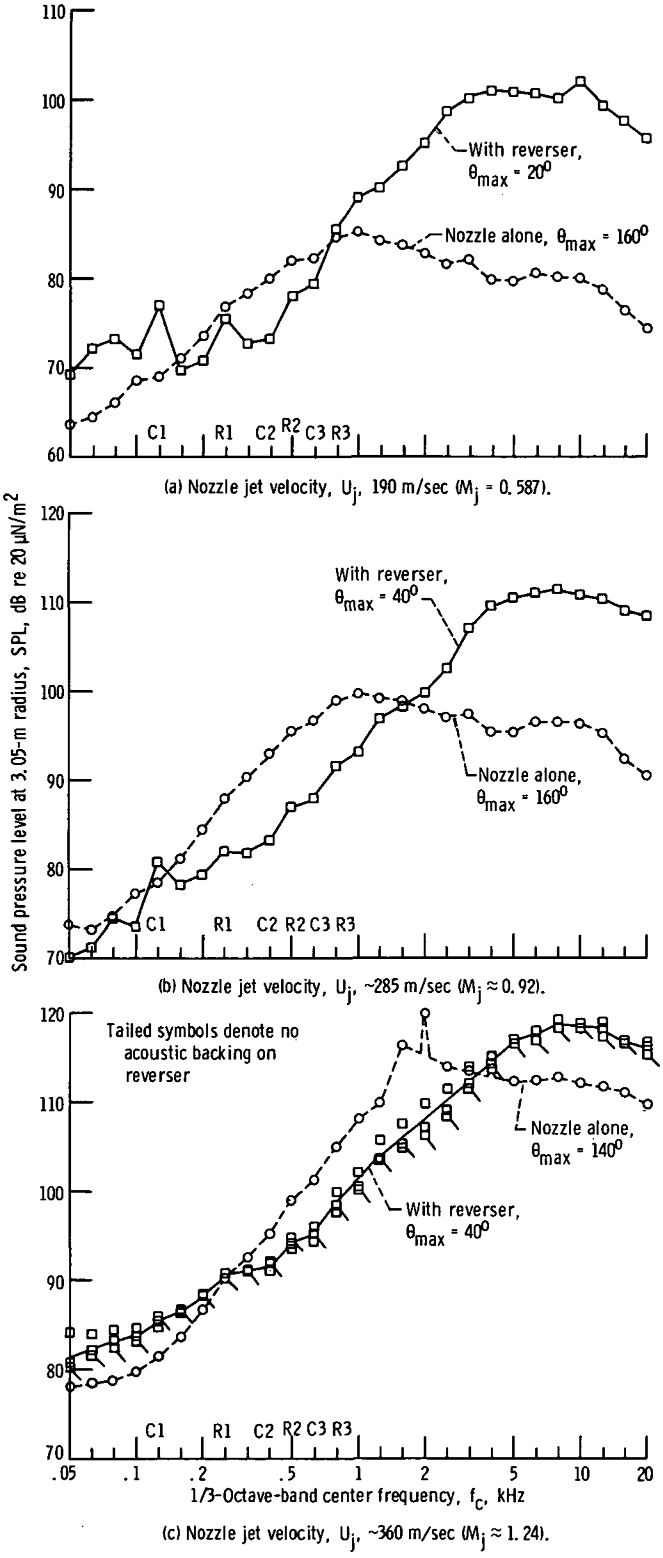

Figure 8. - Effect of thrust reversal on sound-pressure-level spectrum at angle of maximum overall sound pressure level for 2.26- by 11.43-centimeter slot nozzle and V-gutter reverser at various velocities. Normal horizontal position; no offset; spacing ratio, X/D_h, -0.168.

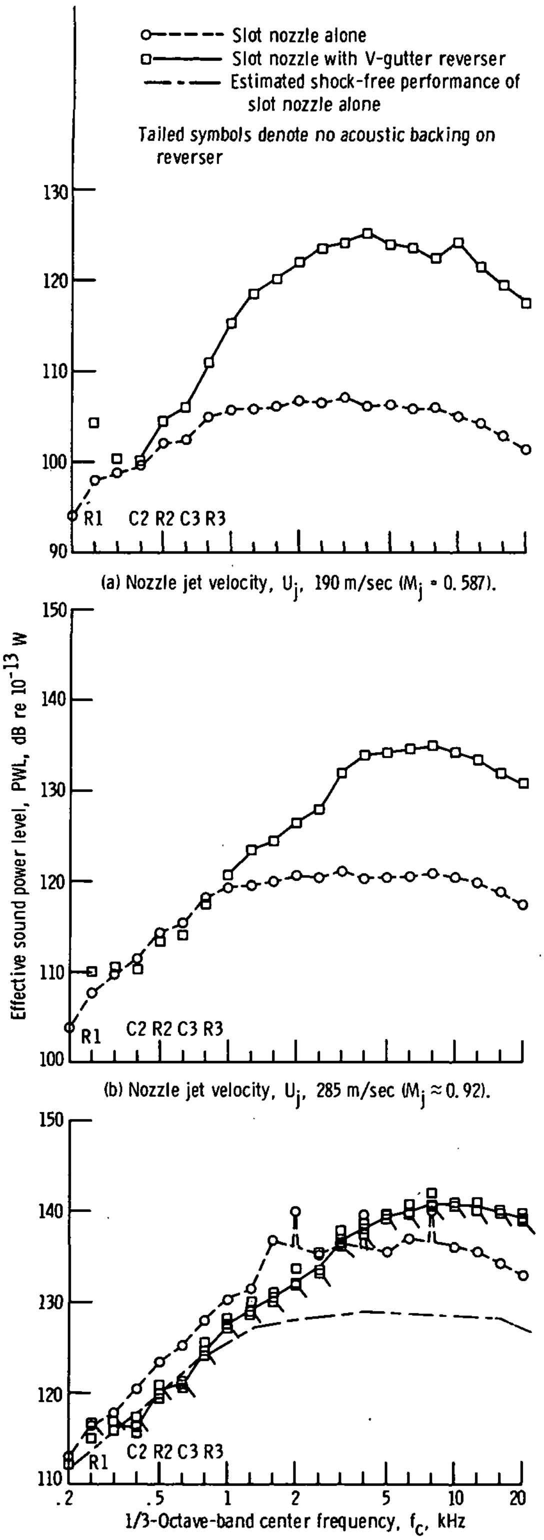

(c) Nozzle jet velocity, U_j, 360 m/sec ($M_j \approx 1.24$).

Figure 9. - Effective sound power level spectra for 2.26- by 11.43-centimeter slot nozzle with and without V-gutter reverser.

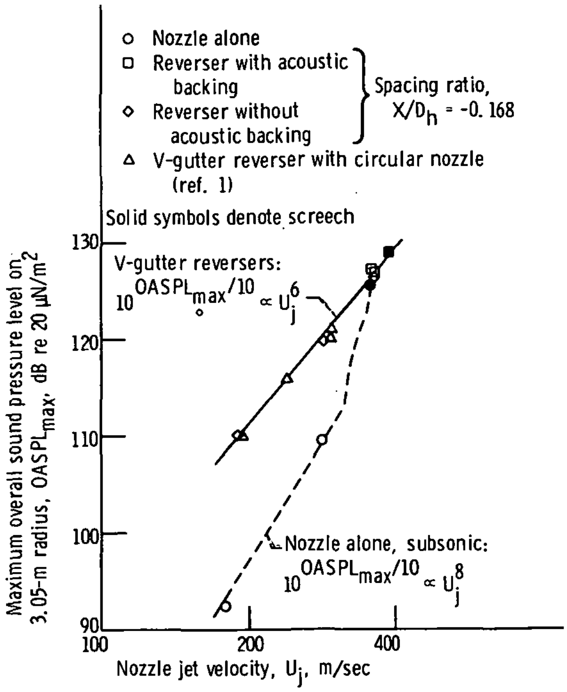

Figure 10. - Effect of velocity on maximum overall sound pressure level for 2.26- by 11.43-centimeter slot nozzle with and without V-gutter reverser and comparison with circular nozzle with V-gutter reverser from reference 1.

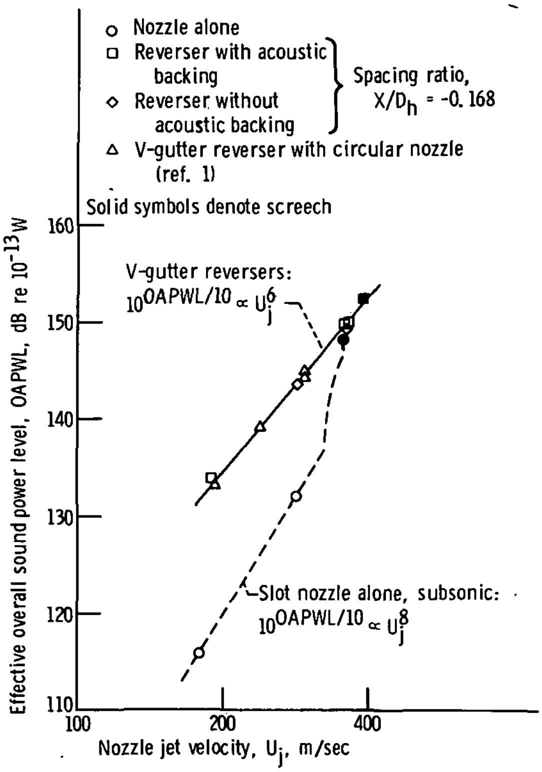

Figure 11. - Effect of velocity on effective overall sound power level for 2.26- by 11.43-centimeter slot nozzle with and without V-gutter reverser and comparison with circular nozzle with V-gutter reverser from reference 1.

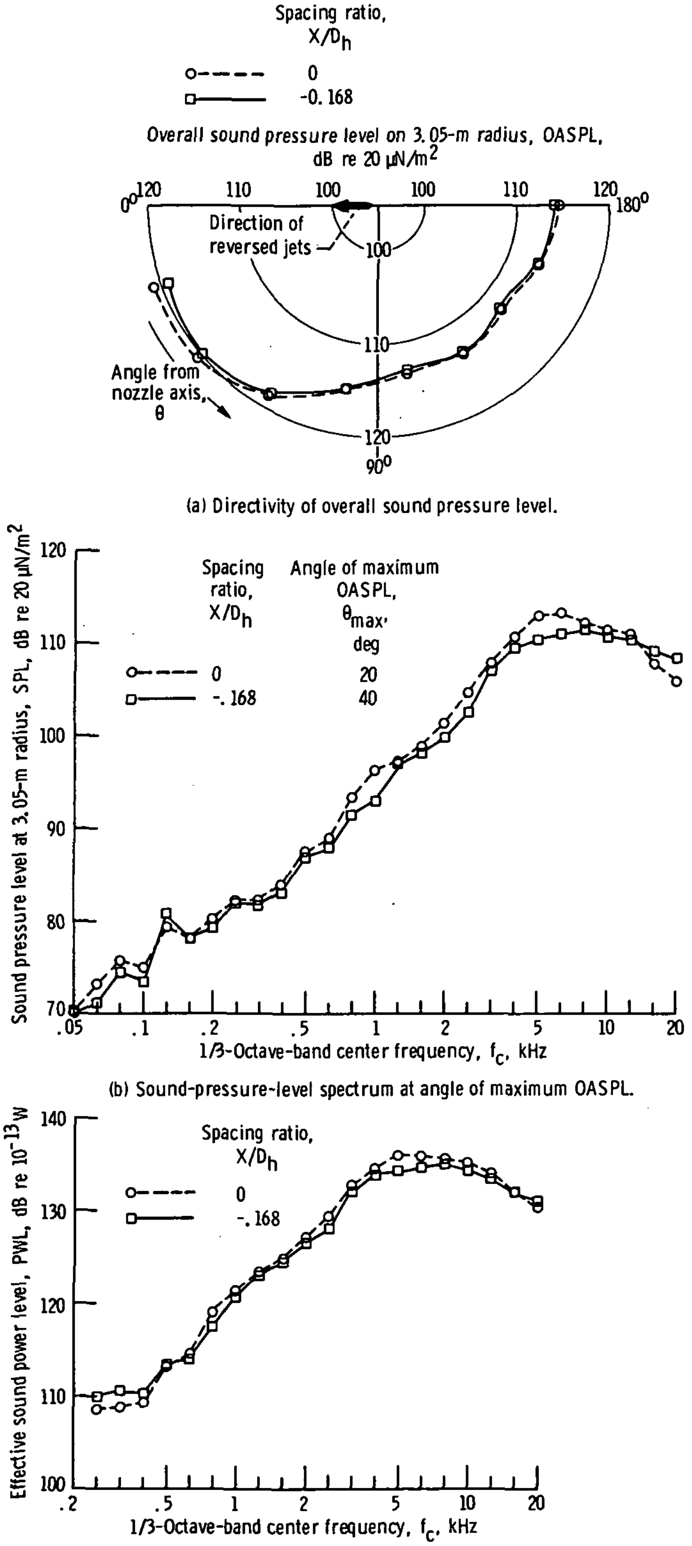

(a) Directivity of overall sound pressure level.

(b) Sound-pressure-level spectrum at angle of maximum OASPL.

(c) Effective sound power level spectrum.

Figure 12. - Effect of reverser-to-nozzle spacing for 2.26- by 11.43-centimeter slot nozzle with V-gutter reverser. Nozzle jet velocity, U_j = 286 m/sec; no acoustic backing.

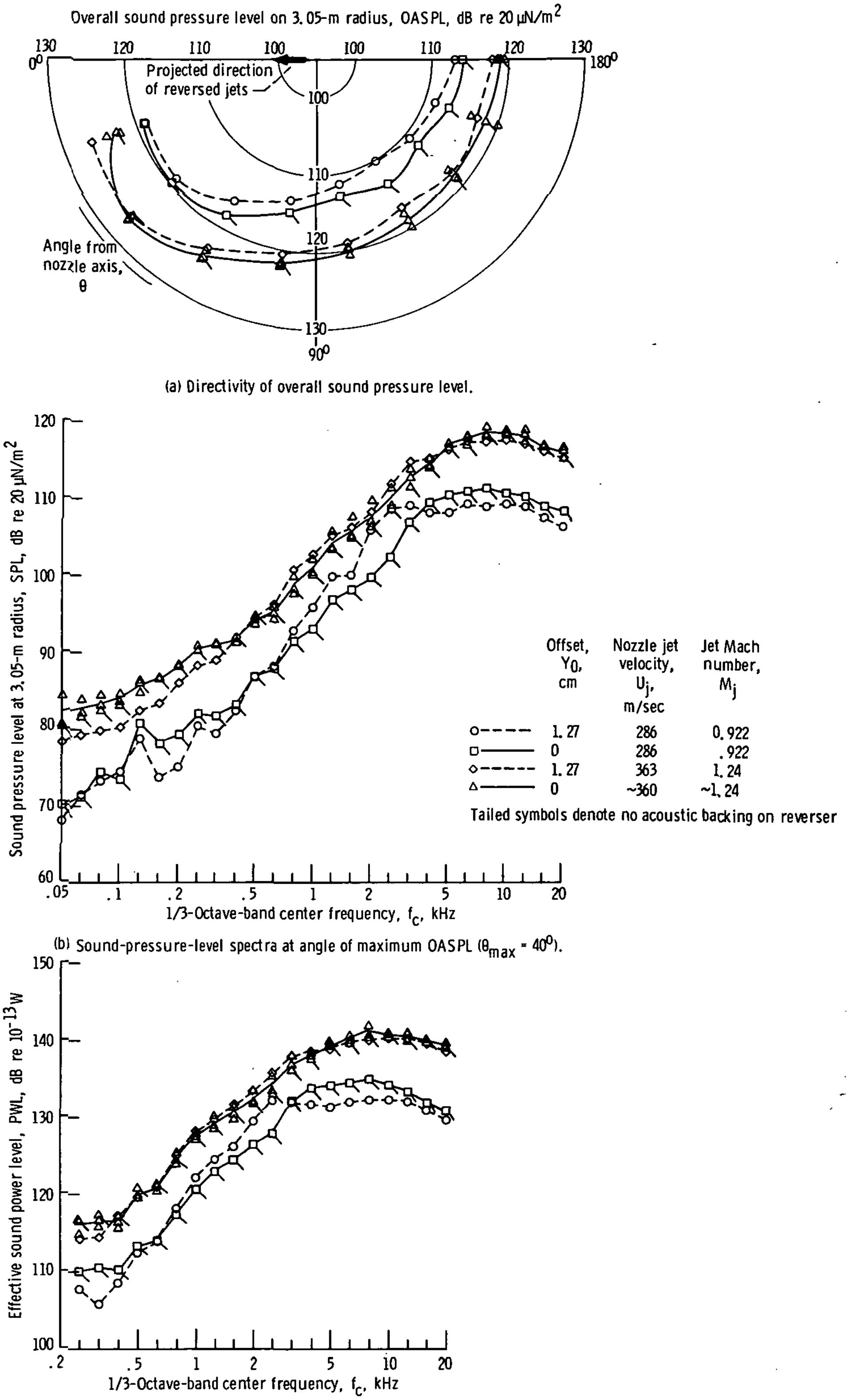

(a) Directivity of overall sound pressure level.

(b) Sound-pressure-level spectra at angle of maximum OASPL (θ_{max} = 40°).

(c) Effective sound-power-level spectra.

Figure 13. - Effect of reverser-to-nozzle offset for 2.26- by 11.43-centimeter slot nozzle with V-gutter reverser.

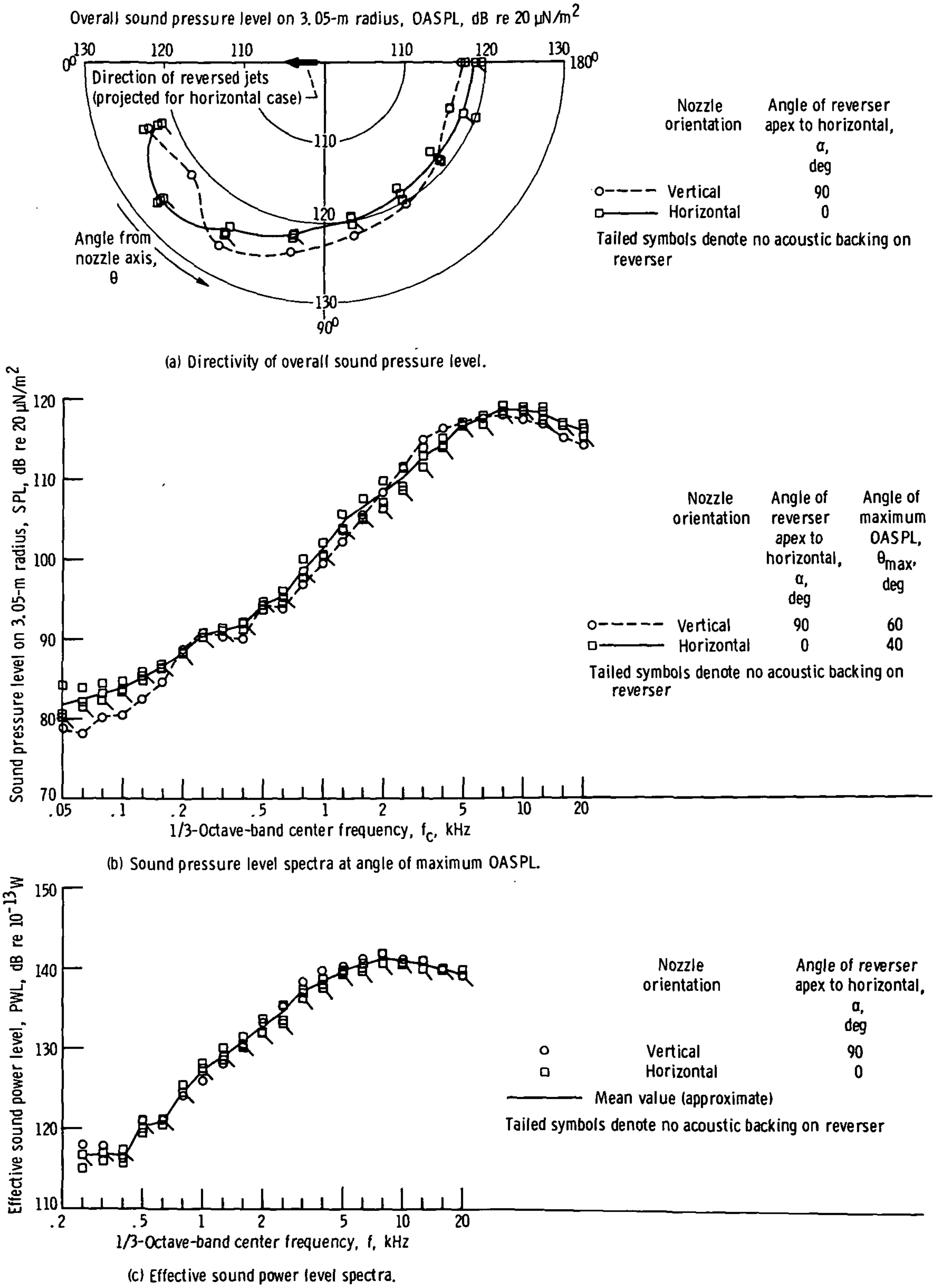

Figure 14. - Effect of orientation for 2.26- by 11.43-centimeter slot nozzle with V-gutter reverser. Nozzle jet velocity, U_j, ~360 m/sec.

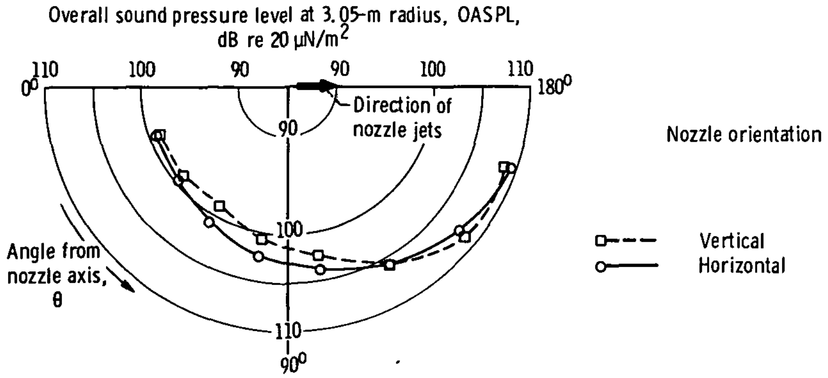

(a) Directivity of overall sound pressure level.

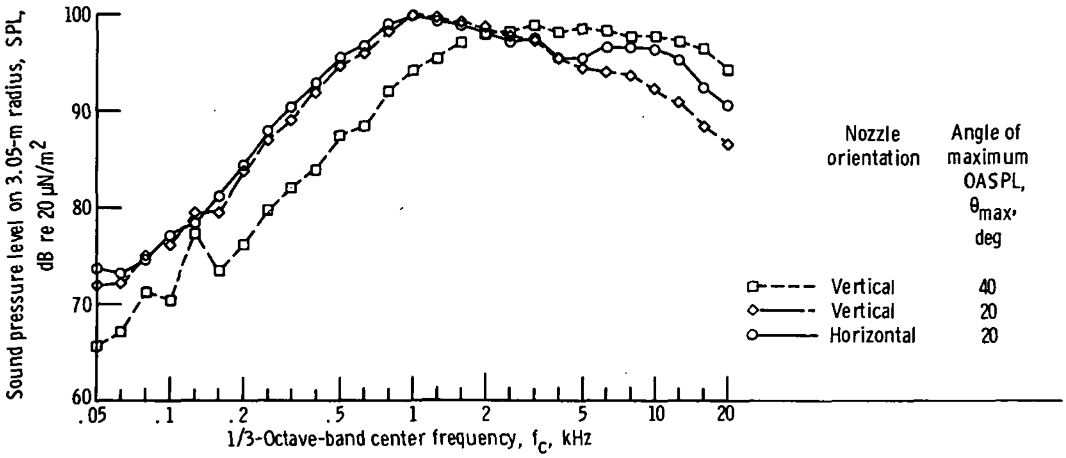

(b) Sound-pressure-level spectra at angle of maximum OASPL.

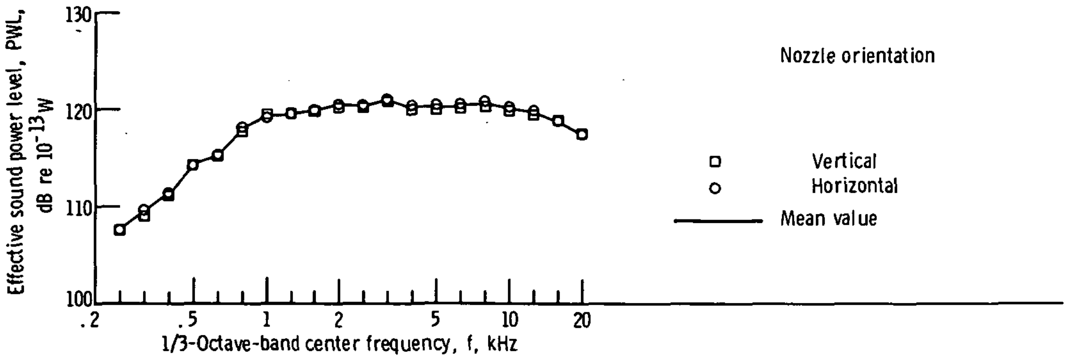

(c) Effective sound-power-level spectra.

Figure 15. - Effect of orientation for 2.26- by 11.43-centimeter slot nozzle. Nozzle jet velocity, U_j, ~285 m/sec.

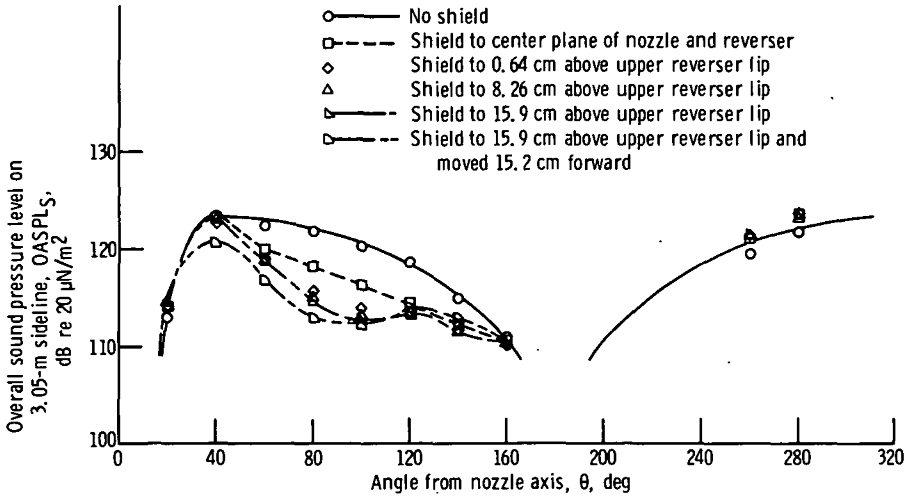

Figure 16. - Effect of shielding on sideline noise; sideline overall sound pressure level as function of angle for 2.26- by 11.43-centimeter slot nozzle with V-gutter reverser. Normal horizontal position; no offset; spacing ratio, X/D_h, -0.168; nozzle jet velocity, U_j, ~357 m/sec.

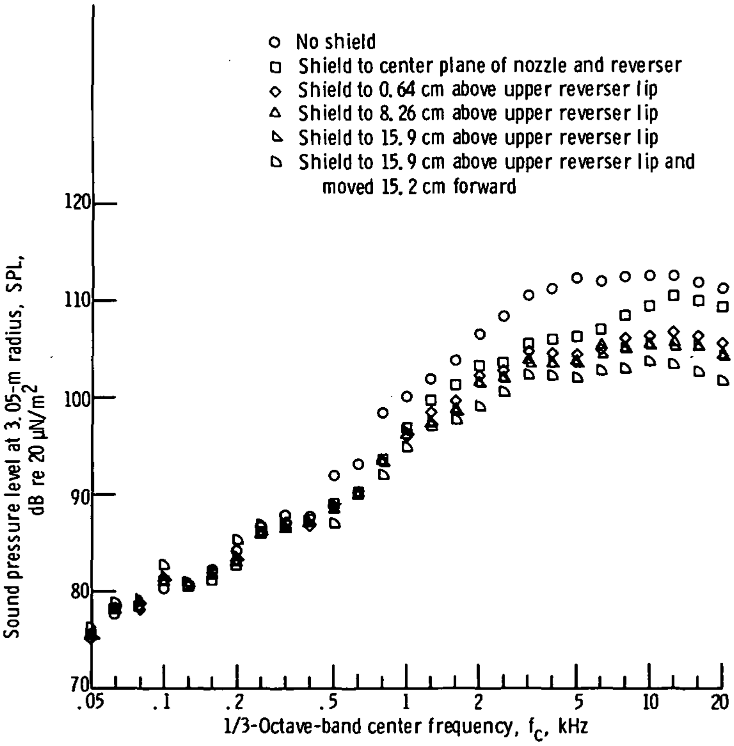

Figure 17. - Effect of shielding on SPL spectra. Angle from nozzle upstream axis, θ, 80°; normal horizontal position; no offset; spacing ratio, X/D_h, -0.168; nozzle jet velocity, U_j, ~357 m/sec.

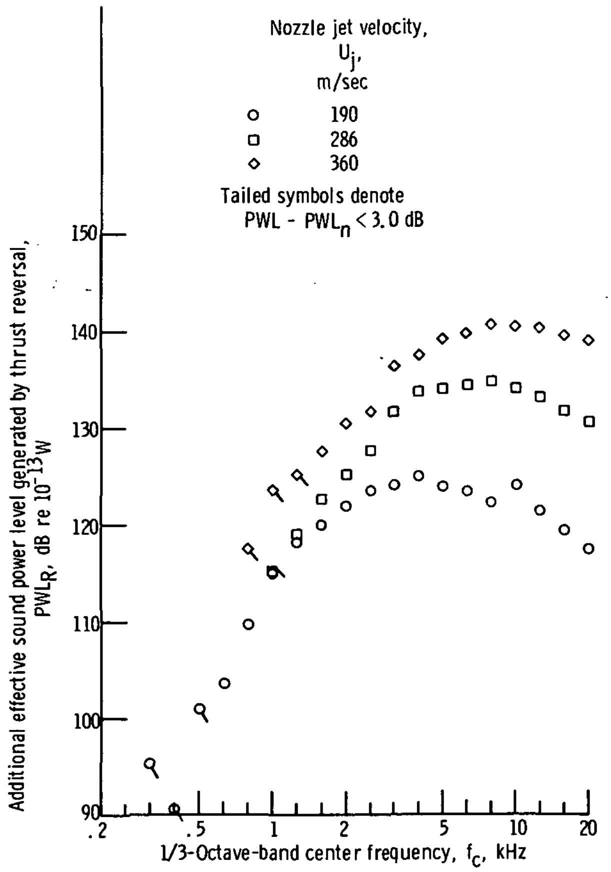

Figure 18. - Sound power level spectra generated by thrust reversal. Normal horizontal position; no offset; spacing ratio, X/D_h, -0.168.

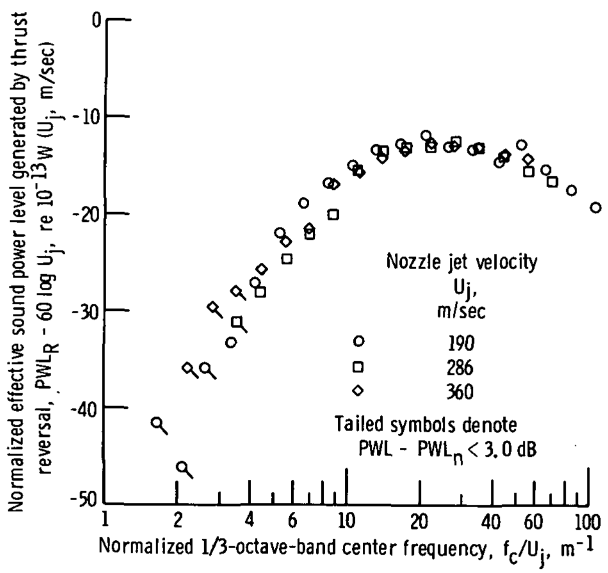

Figure 19. - Normalized power level generated by thrust reversal as function of normalized frequency. Normal horizontal position; no offset; spacing ratio, X/D_h, -0.168.

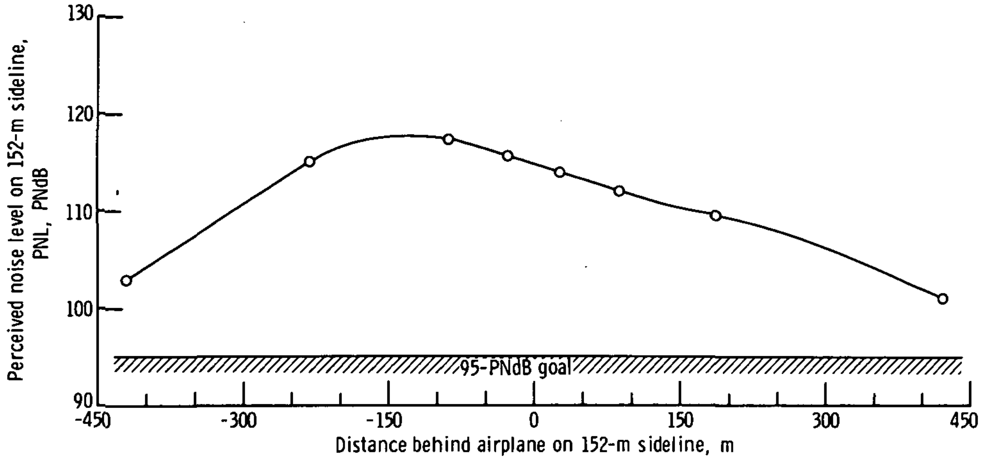

Figure 20. - Sideline noise for wing-slot thrust reversal on 45 400-kilogram augmentor-wing-type airplane. Slot-nozzle pressure ratio, 2.55; jet velocity, U_j, 362 m/sec.

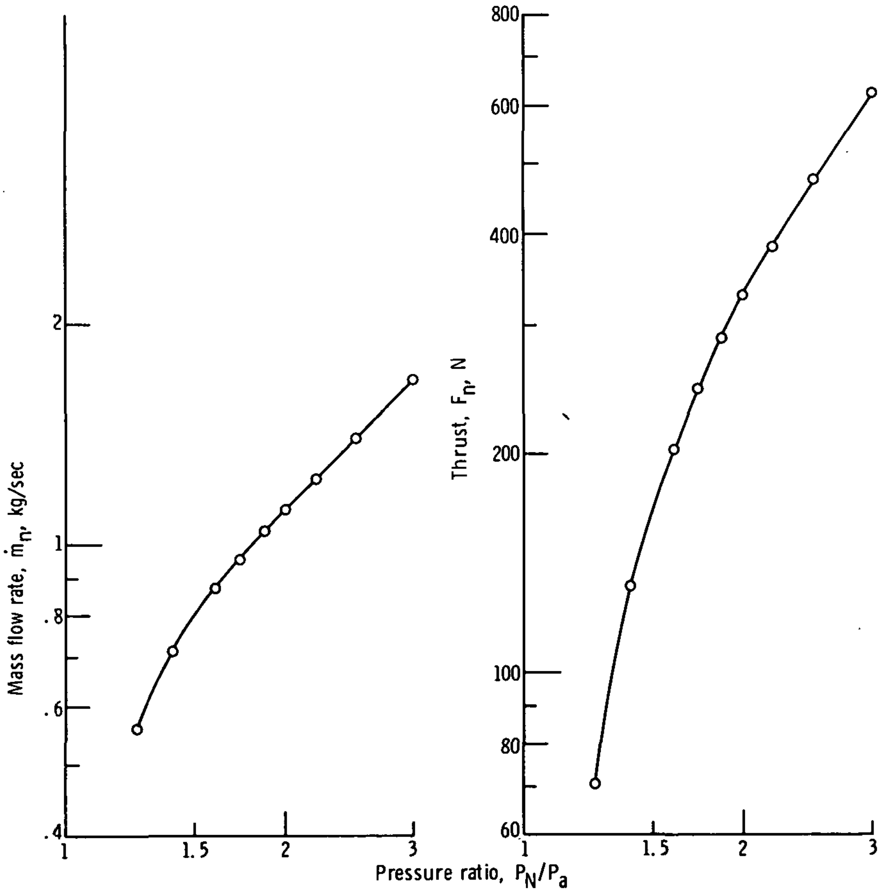

(a) Mass flow rate. (b) Thrust.

Figure 21. - Flow and thrust performance of 2.26- by 11.43-centimeter slot nozzle. Ambient pressure, $P_a \approx 98\ kN/m^2$ abs; nozzle inlet temperature, $T_n \approx 280$ K.

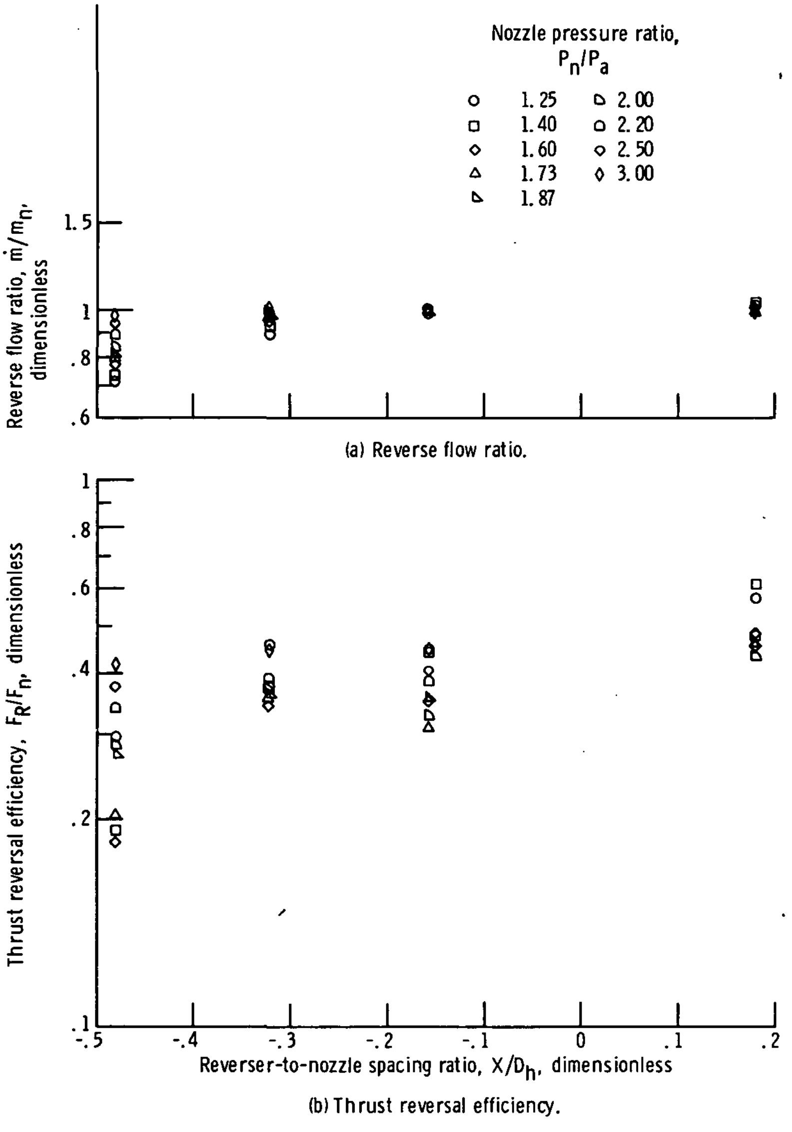

Figure 22. - Effects of spacing on flow rate and reverse thrust for 2.26- by 11.43-centimeter slot nozzle with V-gutter reverser. Ambient pressure, $P_a \approx 98\ kN/m^2$ abs; nozzle inlet temperature, $T_n \approx 280\ K$.

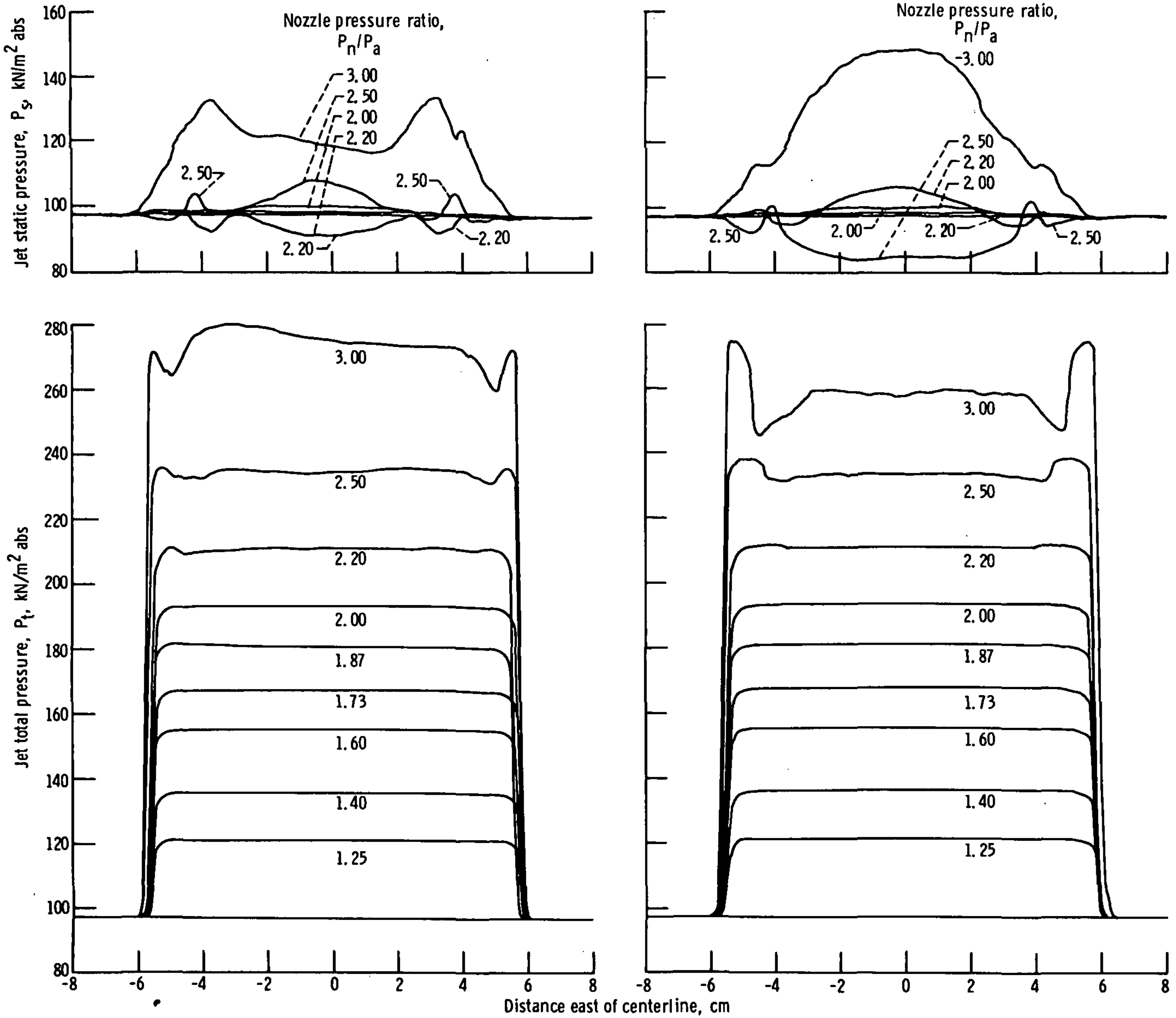

(a) Total-pressure probe 0.64 centimeter downstream of nozzle exit plane.

(b) Total-pressure probe 1.27 centimeters downstream of nozzle exit plane.

Figure 23. - Jet total pressure and static pressure 1.27 centimeters downstream of total as function of distance from nozzle centerline for various pressure ratios. Nozzle and probe travel horizontal.

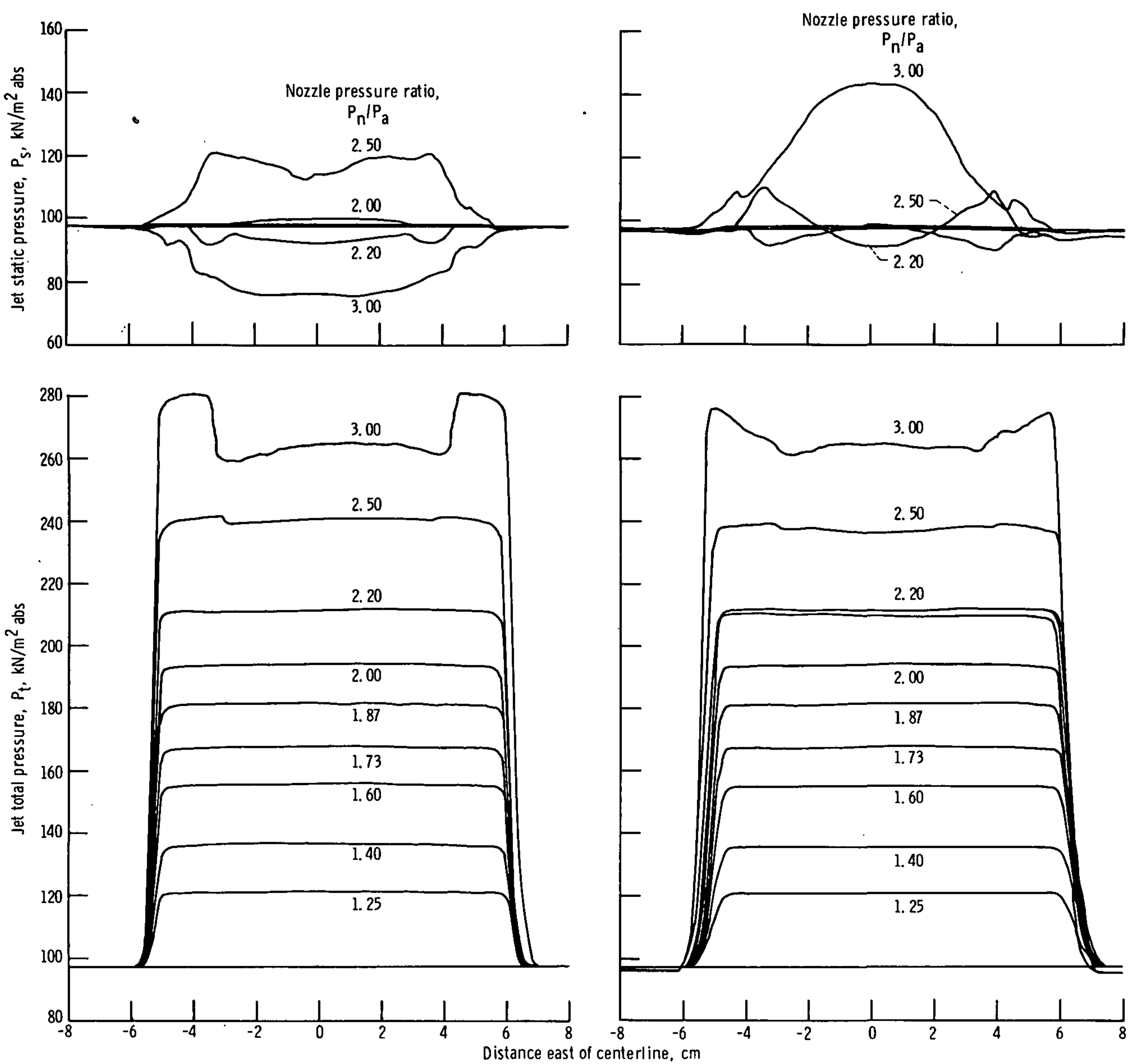

(c) Total-pressure probe 2.54 centimeters downstream of nozzle exit plane.

(d) Total-pressure probe 5.08 centimeters downstream of nozzle exit plane.

Figure 23. - Continued.

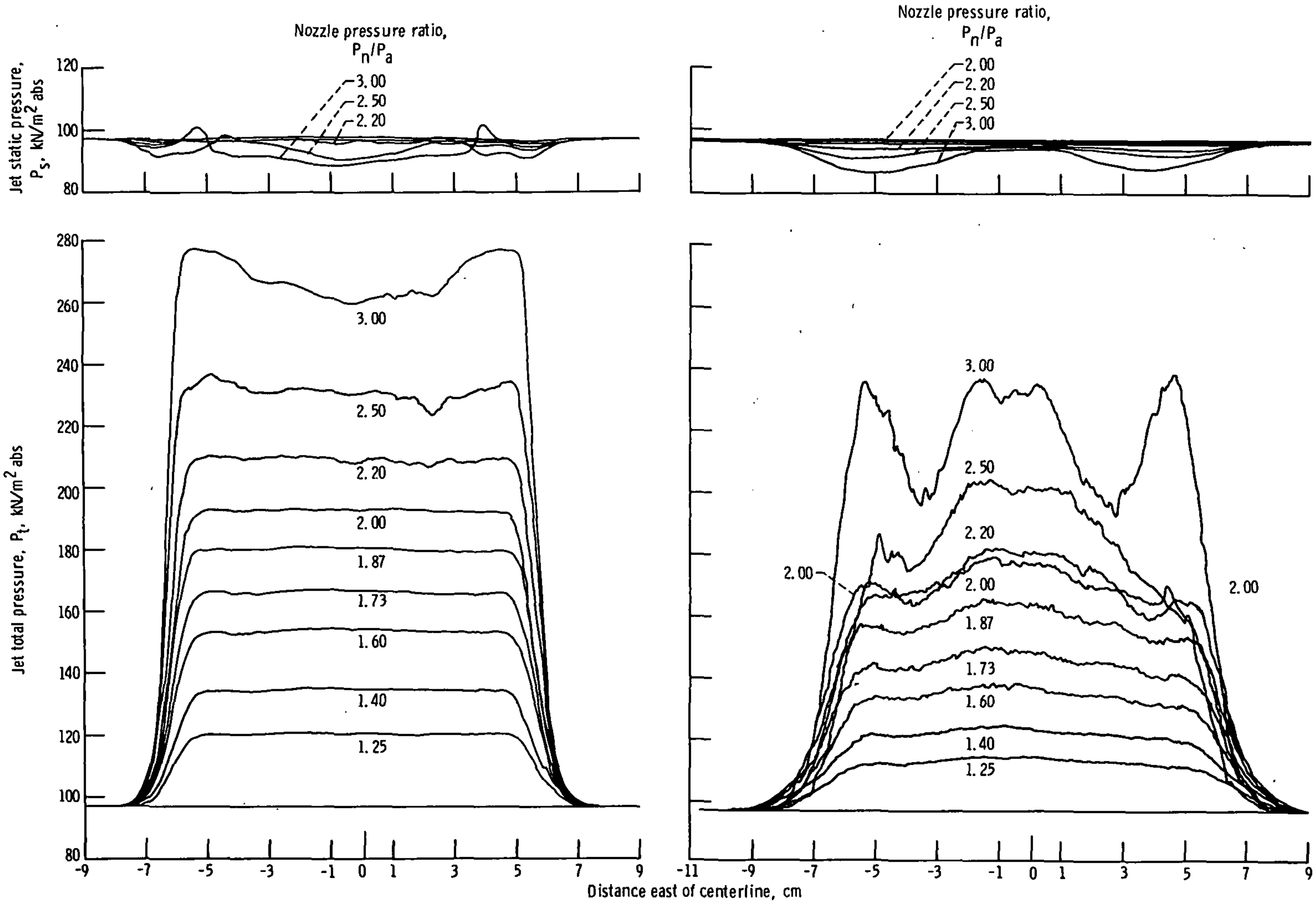

(e) Total-pressure probe 10.16 centimeters downstream of nozzle exit plane.

(f) Total-pressure probe 20.32 centimeters downstream of nozzle exit plane.

Figure 23. - Continued.

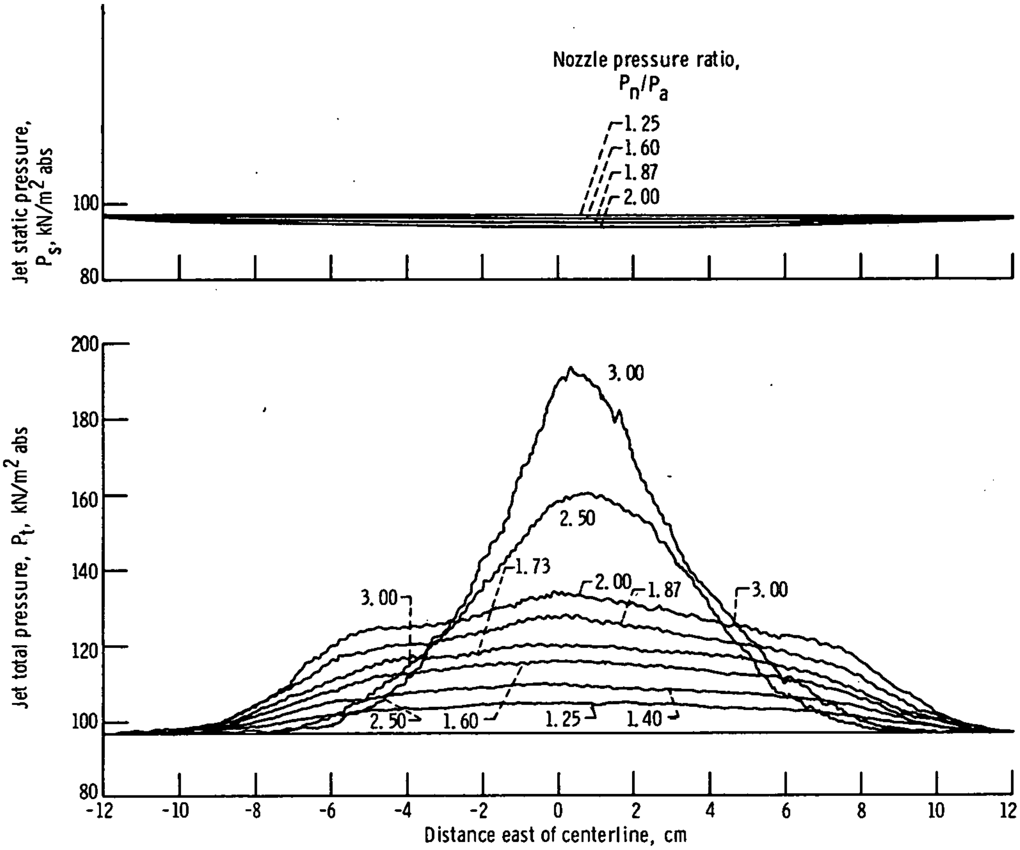

(g) Total-pressure probe 36.8 centimeters downstream of nozzle exit plane.

Figure 23. - Concluded.

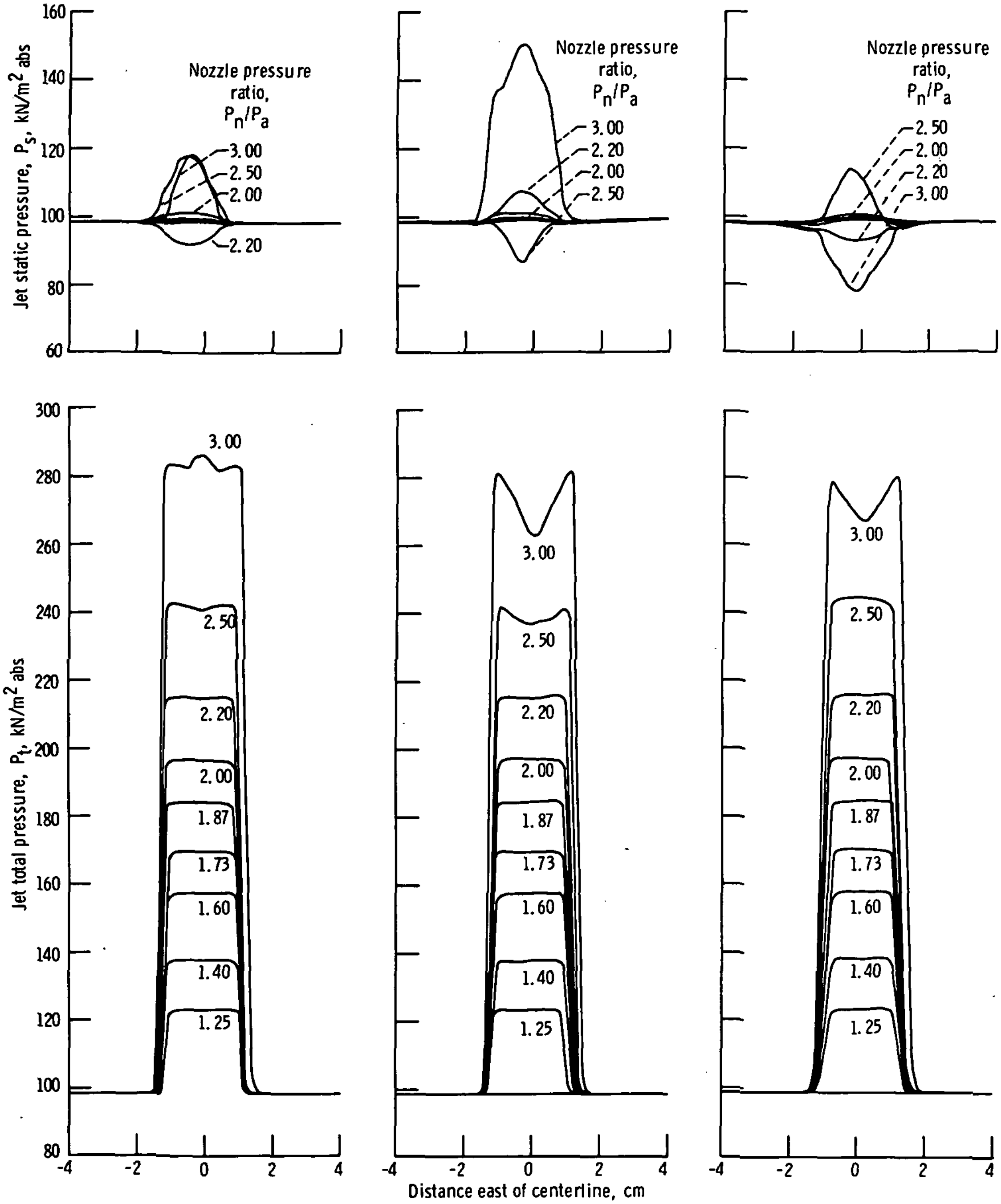

(a) Total-pressure probe 0.64 centimeter downstream of nozzle exit plane.

(b) Total-pressure probe 1.27 centimeters from nozzle exit plane.

(c) Total-pressure probe 2.54 centimeters from nozzle exit plane.

Figure 24. - Jet total pressure and static pressure 1.27 centimeters downstream of total as function of distance from nozzle centerline for various pressure ratios. Nozzle vertical and probe travel horizontal.

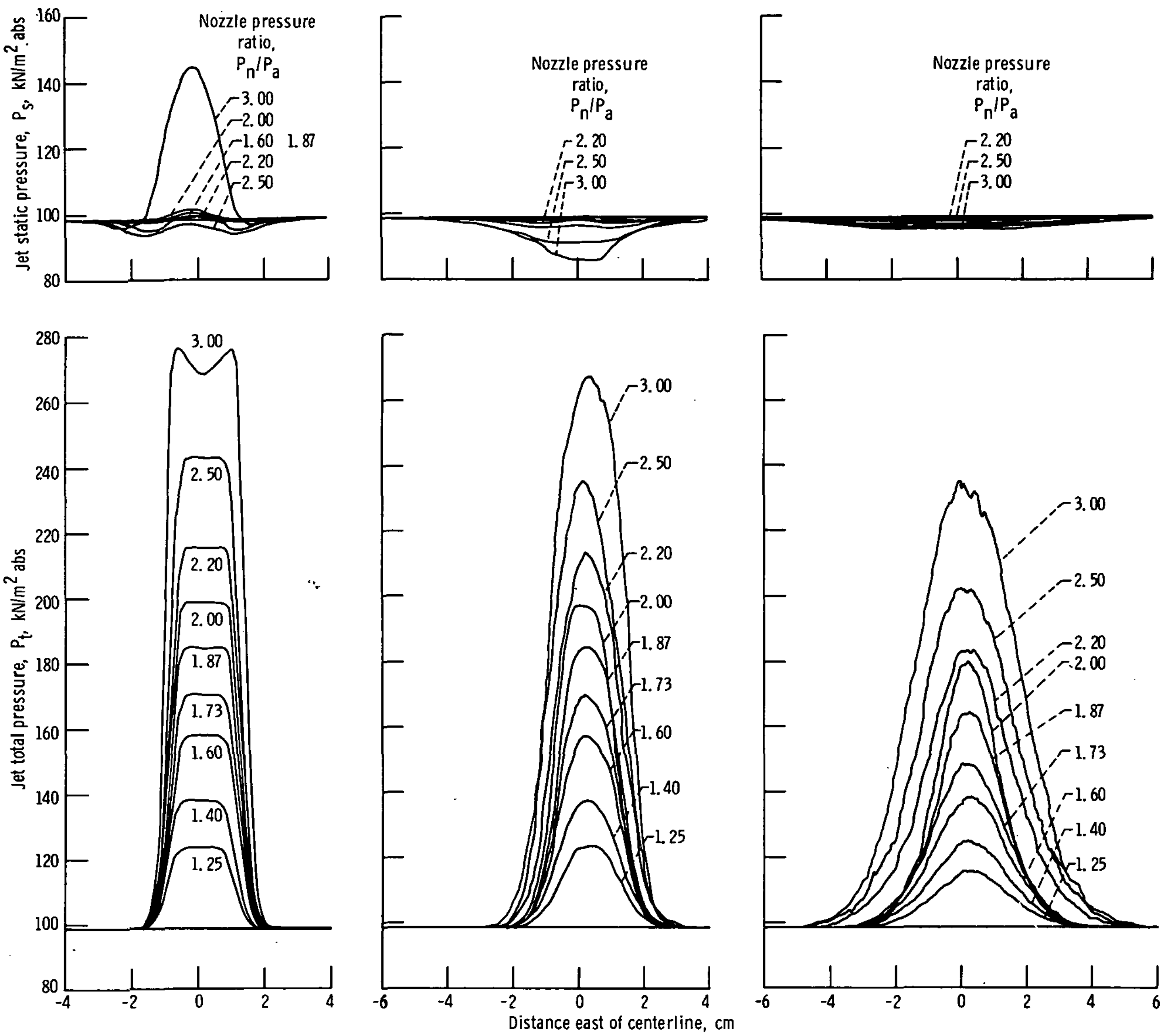

(d) Total-pressure probe 5.08 centimeters downstream of nozzle exit plane.

(e) Total-pressure probe 10.16 centimeters downstream of nozzle exit plane.

(f) Total-pressure probe 20.32 centimeters downstream of nozzle exit plane.

Figure 24. - Continued.

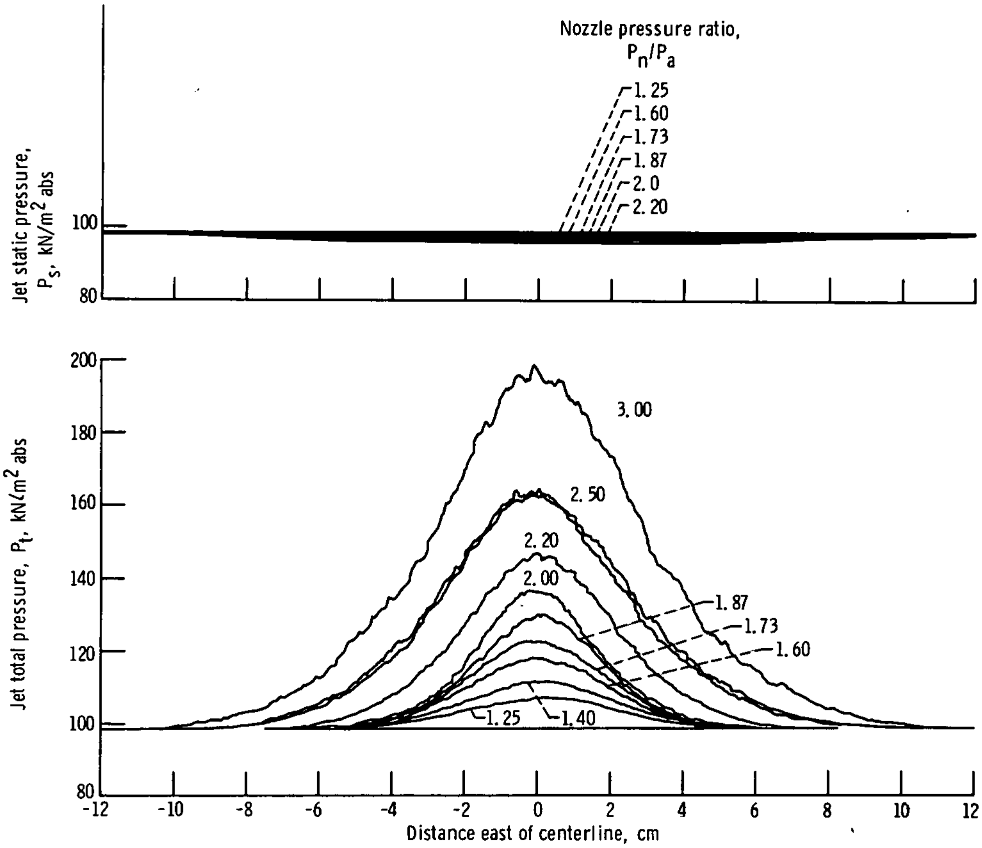

(g) Total-pressure probe 36.8 centimeters downstream of nozzle exit plane.

Figure 24. - Concluded.

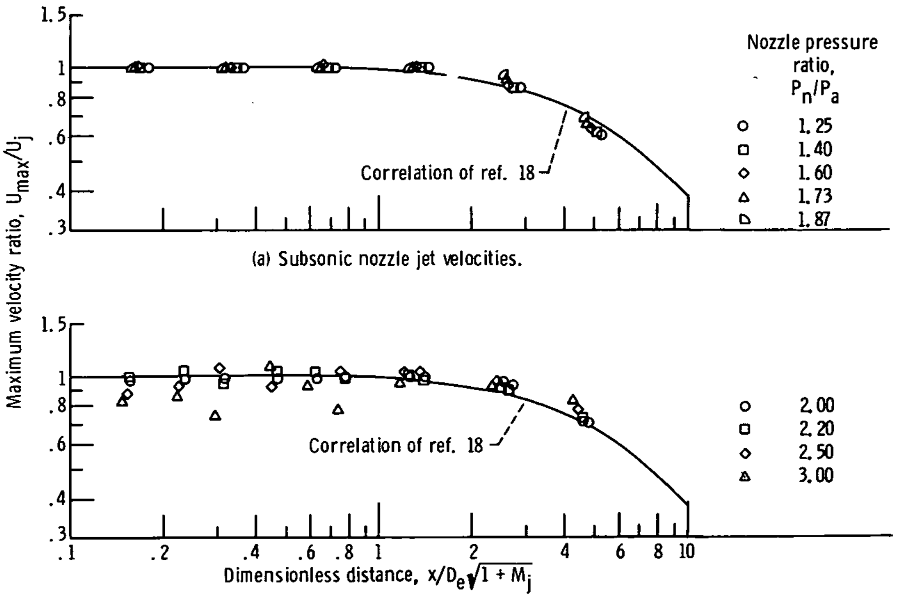

(a) Subsonic nozzle jet velocities.

(b) Supersonic nozzle jet velocities.

Figure 25. - Comparison of maximum velocity decay data for 2.26- by 11.43-centimeter slot nozzle with the correlation of reference 18.

"The aeronautical and space activities of the United States shall be conducted so as to contribute . . . to the expansion of human knowledge of phenomena in the atmosphere and space. The Administration shall provide for the widest practicable and appropriate dissemination of information concerning its activities and the results thereof."

—NATIONAL AERONAUTICS AND SPACE ACT OF 1958

NASA SCIENTIFIC AND TECHNICAL PUBLICATIONS

TECHNICAL REPORTS: Scientific and technical information considered important, complete, and a lasting contribution to existing knowledge.

TECHNICAL NOTES: Information less broad in scope but nevertheless of importance as a contribution to existing knowledge.

TECHNICAL MEMORANDUMS: Information receiving limited distribution because of preliminary data, security classification, or other reasons. Also includes conference proceedings with either limited or unlimited distribution.

CONTRACTOR REPORTS: Scientific and technical information generated under a NASA contract or grant and considered an important contribution to existing knowledge.

TECHNICAL TRANSLATIONS: Information published in a foreign language considered to merit NASA distribution in English.

SPECIAL PUBLICATIONS: Information derived from or of value to NASA activities. Publications include final reports of major projects, monographs, data compilations, handbooks, sourcebooks, and special bibliographies.

TECHNOLOGY UTILIZATION PUBLICATIONS: Information on technology used by NASA that may be of particular interest in commercial and other non-aerospace applications. Publications include Tech Briefs, Technology Utilization Reports and Technology Surveys.

Details on the availability of these publications may be obtained from:

SCIENTIFIC AND TECHNICAL INFORMATION OFFICE

NATIONAL AERONAUTICS AND SPACE ADMINISTRATION

Washington, D.C. 20546